Natural Hazards
and Earth System
Sciences
Open Access
EGU
Discussions

Sensitivity of simulating Typhoon Haiyan (2013) using WRF: the role of cumulus convection, surface flux parameterizations, spectral nudging, and initial and boundary conditions

5   Rafaela Jane Delfino[1,2], Gerry Bagtasa[2], Kevin Hodges[1], Pier Luigi Vidale[1]

[1] Department of Meteorology, University of Reading, Reading, United Kingdom
[2] Institute of Environmental Science and Meteorology, University of the Philippines-Diliman, Quezon City, Philippines

10   *Correspondence to*: Rafaela Jane Delfino (r.p.delfino@pgr.reading.ac.uk or rpdelfino@up.edu.ph)

Abstract. Typhoon (TY) Haiyan was one of the most intense and highly destructive tropical cyclones (TCs) to affect the Philippines. As such, it is regarded as a baseline for extreme TC hazards. Improving the simulation of such TCs will not only improve the forecasting of intense TCs but will also be essential in understanding the potential sensitivity of future intense
15 TCs with climate change. In this study, we investigate the effects of model configuration in downscaling TY Haiyan using the Weather Research Forecasting (WRF) Model. Sensitivity experiments were conducted by systematically altering the choice of cumulus schemes, surface flux options, and spectral nudging. In addition to using the European Centre for Medium-Range Weather Forecasts Re-analysis 5th Generation (ERA5) single high resolution realization as initial and boundary conditions, we also used four of the ten lower resolution ERA5 Data Assimilation System (EDA) ensemble members as initial and
20 boundary conditions. Results indicate a high level of sensitivity to cumulus schemes, with a trade-off between using Kain-Fritsch and Tiedtke schemes that have not been mentioned in past studies of TCs in the Philippines. The Tiedtke scheme simulates the track better (with a lower mean Direct Positional Error (DPE) of 33 km), while the Kain-Fritsch scheme produces stronger intensities (by 15 hPa minimum sea level pressure). Spectral nudging also resulted in a reduction in the mean DPE by 20 km and varying the surface flux options resulted in the improvement of the simulated maximum sustained winds by up to
25 10 ms^{-1}. Simulations using the EDA members initial and boundary conditions revealed low sensitivity to the initial and boundary conditions, having less spread than the simulations using different parameterization schemes. We highlight the advantage of using an ensemble of cumulus parameterizations to take into account the uncertainty in the track and intensity of simulating intense tropical cyclones.

1 Introduction

30 As a country of 109 million people over more than 7,000 islands, the Philippines is considered one of the most natural hazard-prone countries in the world (Brucal et al., 2020) and is ranked in the top five of all countries in terms of exposure to climate-related risks (Eckstein et al., 2020). One of the most important hazards the Philippines is exposed to is tropical cyclones (TCs). TCs bring intense winds, extreme precipitation, and storm surges that affect a large portion of the Philippine population (Bagtasa, 2017; Lyon and Camargo, 2009). Due to its location in the western North Pacific Ocean, where TC formation is
35 conducive all year, the Philippines is exposed to an average of 10 landfalling TCs annually (Cinco et al., 2016). Since 1990, TCs in the Philippines have resulted in up to half of the total losses from all natural disasters amounting to about USD 20 billion in damages (Brucal et al., 2020) and an annual average death toll of 885 with estimated accumulated deaths due to TCs of approximately 30,000 from 1980 to 2013 (Yonson et al. 2016). It is estimated that about 5 million people are affected annually or over 570,000 are affected on average per destructive TC (Brucal et al., 2020).

40

One of the strongest typhoons that made landfall in the Philippines in recent history is Typhoon (TY) Haiyan (locally named "Yolanda"), which is considered the second costliest Philippine TC since 1990 (EM-DAT, 2020) and one of the deadliest since the 1970s (Cinco et al., 2016; Lander et al., 2014; Lagmay et al., 2015). TY Haiyan was a category-5 super typhoon that claimed the lives of at least 7,300 people, most of them from drowning due to the devastating 5 to 7-meter-high storm surge

45   and coastal inundation (Soria et al., 2016). It also affected more than 16 million people (NDRRMC, 2014) and caused an estimated USD 5–15 billion worth of damage particularly in agriculture and critical infrastructure (Brucal et al., 2020). Comiso et al. (2015) found that TY Haiyan coincided with the warmest sea surface temperature (SST) observed over the Pacific warm pool region which may have contributed to its intense nature. This relation between intense TCs and warmer tropical SSTs, has also been found in the Atlantic (Emanuel 2005), and suggests that continuous warming may lead to more intense TCs in

50   the future. Consistently, an increasing trend in intense TC frequency affecting the Philippines since the 1970's has been observed (Cinco et al. 2016; Comiso et al. 2015). TC rainfall is also expected to increase in the future as TCs intensify (Intergovernmental Panel on Climate Change, 2021; Patricola and Wehner 2018), potentially increasing the risk of flooding and landslides. Given TY Haiyan's intensity and impacts, it is regarded as a benchmark for an intense and destructive TC. Hence, it is important to test how well it can be simulated in current models in the present climate and what are the sensitivities

55   to model formulation. Improving the representation of intense TCs like Haiyan in regional climate models (RCMs) such as the Weather Research and Forecasting (WRF) model (Skamarock et al. 2008) is essential for simulations of such TCs in different future climate change scenarios to provide credible impact assessments.

While global climate models (GCMs) are very useful for looking at the changes in TC activity under different climate change

60   scenarios (e.g. frequency, intensity, genesis from a climatological and global/regional perspective) (Gallo et al., 2019; Villafuerte et al.; 2021, Patricola and Wehner 2018) and some advances have been made in the past few decades in the use of global convection-permitting models (Judt et al., 2021), previous studies still demonstrate the need for (convection-resolving/convection-permitting) RCM simulations to better simulate the processes relevant to the TC formation and development as well as their properties, particularly the most intense ones (e.g. Walsh et al., 2013). In consideration of the

65   computational cost in resolving important TC processes, the use of RCMs is a valuable and complementary approach to using GCMs in investigating the potential changes in TCs in the future. One such RCM is the WRF Model (Skamarock et al. 2008) which is currently used for operational forecasting by the country's meteorological office - Philippine Atmospheric, Geophysical and Astronomical Services Administration (PAGASA) (Flores 2019; Aragon and Pura 2016) and also used in studies projecting future changes in temperature and rainfall over the Philippines (Cruz et al., 2016; Daron et al., 2018;

70   Tolentino and Bagtasa, 2021).

A consensus of past modelling studies of western North Pacific TCs, including TY Haiyan, show the cumulus convection scheme as having the most influence on its intensity over other model parameters such as the planetary boundary layer (PBL) and/or microphysics schemes (Islam et al. 2014; Di et al. 2019). In particular, the Kain-Fritsch (KF) (Kain, 2004) cumulus

75   convection scheme has been found to produce the best TC tracks and wind intensity estimates (Shen et al., 2019; Zhang et al., 2011; Spencer and Shaw, 2012; Prater and Evans, 2002; Mohandas and Ashrit, 2012). Furthermore, the often-selected KF scheme was shown to be also sensitive to model resolution (Li et.al., 2018). However, the use of the KF scheme has also shown certain limitations. A study by Torn and Davis (2012) found that the KF scheme produces larger TC track biases than the Tiedtke (TK) cumulus convection scheme. Other than the said parameterization schemes, improvements in simulations of

80   TC intensity are also found to be influenced by the surface flux options (Kueh et al., 2019).

In this paper, we revisit the simulation of TY Haiyan using downscaling and assess its sensitivity to model formulation and the driving initial and boundary conditions in preparation for pseudo-global warming and CMIP6 climate projection

85   experiment studies. This study builds on the work of Islam et al. (2015) who assessed the effects of different combinations of Planetary Boundary Layer, microphysics and cumulus convection scheme using WRF but found substantial underestimation of TY Haiyan's intensity regardless of the sensitivity to physics parameterization; Li et al. (2018) who used WRF to look at the effects of the cumulus parameterization at different resolutions (9-2 km) and found that the most effective resolution to simulate TY Haiyan with no cumulus parameterization or a revised KF scheme is at 2-km and 4-km resolution, respectively;

90   and that of Kueh et al. (2019) who looked at the influence of the different surface flux options in simulating TY Haiyan's intensity using one cumulus convection scheme and found that a better representation of surface flux formulas improved the simulated intensity in WRF. Here, we investigate the effects of the different combinations of model cumulus convection schemes, spectral nudging and surface flux options on the TY Haiyan track, intensity and rainfall simulations. From this study the best combination is determined which will then be used for investigating the effects of future climate change on TY Haiyan and other TC cases. The associated storm surge of TY Haiyan (Mori et al. (2014), Nakamura et al. (2017) and Takayabu et

95   al. (2015) is not considered here. Model parameterization scheme sensitivity studies that assess the simulation of TCs provide guidance to future TC modelling studies (Villafuerte et al., 2021). This study also seeks to contribute to such studies with a particular focus on the Philippines by assessing the skill and sensitivity of a TC case study using a mesoscale numerical weather prediction model. In particular, it aims to study the influence of the combination of cumulus convection scheme and the different surface flux options to the different TC characteristics. This study adds on existing literature by looking at the effects

100   of cumulus convection schemes combined with different flux options and spectral nudging. Specifically, it aims to address the following questions:

- How sensitive are the TY Haiyan simulations to convective schemes, surface flux options and spectral nudging?
- How sensitive are the simulated track and intensity of TY Haiyan to the uncertainty in the initial and boundary conditions?

105

The results will provide valuable information for regional climate downscaling of intense TCs, which can be used in evaluating the sensitivity of future TCs in climate change simulations. Section 2 provides a description of the methodology. Then the paper continues with the results of the sensitivity experiments followed by the discussion, and finally, Section 4 provides a summary of the findings and recommendations for future work.

110   **2 Method**

2.1 Case Study: Typhoon Haiyan Brief Description

Typhoon Haiyan originated from an area of low pressure near the Federated States of Micronesia (157.2°E, 5.8°N) on November 2, 2013, and moved westward forming into a tropical storm on November 2, 2012. Typhoon Haiyan formed in an environment with a significantly high SSTs (peaking at 30.1°C in November 2013), which was considered the highest observed

115   during the period between 1981 to 2014 in the Warm Pool Region (Comiso et al 2015). It then rapidly intensified into a TY on November 5 at 142.9°E, 6.9°N and was classified as a category-5 equivalent super typhoon by the Joint Tropical Warning Center (JTWC) and was classified as a Typhoon by PAGASA, its highest classification at the time. It further intensified before making landfall on November 7 2040 UTC. It traversed the central section of the Philippines and started to slowly weaken to a tropical depression on November 11 (JMA, 2013). Typhoon Haiyan claimed the lives of more than 7,300 people, mostly due

120   to the associated storm surge and coastal inundation. It is estimated to have caused between USD 5-15 billion worth of direct damages in agriculture and infrastructure (Brucal et al., 2020) and affected more than 16 million people (NDRRMC 2014).

2.2 Model Description

Simulations were conducted using WRF version 3.8.1 (Skamarock et al. 2008), a non-hydrostatic numerical weather prediction
RCM developed by the National Center for Atmospheric Research (NCAR). It is used for atmospheric research and operational
forecasting, and increasingly for regional climate research (Powers et al., 2016). The model includes a variety of physical
parameterization schemes, including cumulus convection, microphysics, radiative transfer, planetary boundary layer, and land
surface. The WRF Advanced Research WRF (WRF-ARW) solver uses the Arakawa-C grid as the computational grid and the
Runge-Kutta 3rd order time integration schemes (MMML-NCAR, 2019). Skamarock et al. (2008) provides a more detailed
description of the model specifications. PAGASA uses WRF for its operational forecasting over the Philippine Area of
Responsibility (Flores 2019; Aragon and Pura 2016) and it is also used in studies projecting future changes in temperature and
rainfall over the Philippines (Cruz et al., 2016).

The land surface information comes from the 30 arc s (*1 km) resolution Moderate Resolution Imaging Spectroradiometer
(MODIS) satellite dataset with 20 global land use categories.

2.3 Initial and boundary conditions

The European Centre for Medium-Range Weather Forecasts (ECMWF) Re-analysis 5th Generation (ERA5) data is used for
both the initial and boundary conditions. It is the latest generation of reanalysis products produced by ECMWF with horizontal
resolution of 31 km, hourly temporal resolution and 137 vertical levels (Herbatsch et al., 2020). ERA5 uses observations
collected from satellites and in-situ stations, which are quality controlled and assimilated using 4D-VAR, a model based on
the ECMWF's Integrated Forecast System (IFS) Cycle 41r2.

Alongside the release of the ERA5 single realisation deterministic data from 1979 to the present, data from the Ensemble of
Data Assimilations (EDA) system was also made available. The EDA system is a 10-member ensemble at a lower resolution
than the deterministic data (60 km horizontal resolution and 3-hourly) (Hennermann, 2018). The EDA system provides
estimates of analysis and short-range forecasts through one control and nine perturbed members, which provide background
error estimates for the deterministic forecasts. This system allows for estimating uncertainty since it provides estimates of the
analysis and short-range forecast. These are provided as an uncertainty measure, albeit with half the resolution of the reanalysis.
To test the sensitivity to varying boundary conditions, simulations were also performed using four randomly selected
representatives of the 10-member ERA5 EDA system. The selected ensemble members were used to test the sensitivity to
different perturbed observations, sea surface temperature fields and model physics the (Isaksen et al., 2010).

2.4 Design of sensitivity experiments and analysis

In this study, the WRF–ARW model has been configured with two nested domains centered over the point of 18.3° latitude,
135° longitude. The outermost grid has 294 x 159 grid points with 25-km grid spacing, while the innermost domain has 745 x
550 grid points with 5-km grid spacing, with 28 vertical levels and the model top pressure level was set to 50 hPa. This model
resolution was chosen in favour of using supercomputing resources for the systematic testing of different parameterization
schemes, and in consideration of additional simulations under future climate conditions. Different domain configurations were
tested prior to selecting this particular configuration, with the current domain configuration having the track and intensity
closest to that observed (not shown). Additional simulations using convection-permitting resolution (single domain, 4.5km)
were also performed and showed no significant change in simulated intensity from the configuration used here (not shown).
The model domain set-up is shown in Fig. 1.

165 In performing the experiments, WRF was run for a 174-hour period from 00 UTC 4 November 2013 – 12 UTC 11 November 2013 to cover the main part of the life cycle of TY Haiyan. Simulations with different start times were conducted (not shown) to sample the different stages in TY Haiyan's lifetime and different initializations. Starting times tested include 4 November 2013 at 00 and 12 UTC, 5 November 2013 at 00 and 12 UTC, 6 November 2013 at 00 and 12 UTC, and 7 November 2013 at 00 UTC. The simulation that started on 4 November 00 UTC was found to be optimal in terms of track and intensity, thus the

170 initialization time of all experiments was fixed at 4 November 2013 00 UTC. For the purposes of this paper, the analysis of the experiments covered only the 72-hour period between 18 UTC 5 November 2013 to 18 UTC 8 November 2013 to cover TY Haiyan's mature stage.
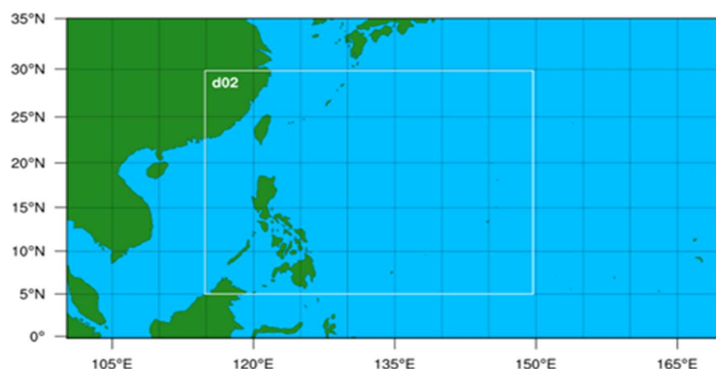
175 **Figure 1: Study domain set-up. The outer 25-km resolution (△x) domain is bounded by 0-170 degrees East and 0-35 degrees North while the inner 5-km resolution (△x) domain is bounded by 115-150 degrees East and 5-28 degrees North.**

Convection is mostly simulated in models with resolution coarser than 10-5km through the cumulus parameterization scheme. WRF's cumulus parameterization scheme simulates the effects of cumulus convection on heat, moisture, and precipitation at

180 the sub-grid scale (Skamarock et al. 2008). The choice of cumulus parameterization schemes has an impact on WRF's ability to simulate the TC track, intensity, and structure (Zhang et al., 2011; Shepherd and Walsh 2016; Parker et al., 2017). Only two schemes were investigated in this study the KF scheme and TK scheme, the difference of which are summarized below in Table 1. These cumulus schemes are used because PAGASA uses KF for its operational forecasting configurations (Flores 2019). It has also often been used for TC simulation studies in the Philippines and has been found, in several studies, to be the

185 best choice for simulating TC track and intensity (e.g. Sun et al., 2019; Li et al., 2018) and rainfall (e.g. Cruz et al., 2016). The TK scheme, on the other hand, has been suggested to be the more appropriate cumulus scheme in tropical weather/climate applications of the WRF model (Parker et al., 2017).

Using a mass flux approach with downdraft removal, and utilizing Convective Available Potential Energy (CAPE), KF is a

190 deep and shallow convection sub-grid scheme that includes clouds, rain, ice, and snow detrainment and cloud persistence (Kain 2004). Although KF can account for relatively small-scale processes that drive convection, it has inherent limitations in simulating shallow convection over tropical oceans (Parker et al., 2017). On the other hand, the TK scheme assumes that the moisture flux through the cloud base is equivalent to the surface moisture flux, as well as momentum transport, cloud detrainment, and ice detrainment (Tiedtke 1989; Zhang et al., 2011). According to Parker et al. (2017), the TK scheme is more

195 appropriate for simulating intense TCs in tropical oceans.

Table 1: Description of the cumulus schemes used in this study

	Kain-Fristch (KF) (Kain, 2004)	**Tiedtke (TK)** (Tiedtke 1989, Zhang et al., 2011)
Type of scheme	Mass-flux	Mass-flux
Cloud detrainment	Yes	Yes
Closure	CAPE Removal	CAPE / Moisture convergence
Triggering mechanism	Controlled by large scale velocity in the vertical direction	Convection is triggered if the parcel is warmer than its surroundings by 0.5K if the parcel is very close to the surface
Cloud radius	Variable	Fixed
Shallow convection	Activates shallow convection when the criteria for deep convection are satisfied	Assumes that the cloud base moisture flux is equal to the surface moisture flux

Sources: Adenyi et al., (2019), Torn and Davis (2012), Shepherd and Walsh (2016)

200

Experiments were also conducted to examine the sensitivity to the available parameterizations for surface flux options. For TC applications, WRF-ARW provides three different formulations of aerodynamic roughness lengths of the surface momentum and scalar fields as surface flux options (isftcflx = 0,1, and 2) (see Kueh et al. 2019 for a detailed description of the differences between these options). It has been shown that surface fluxes can influence the model's ability to simulate TC

205 intensity and structure (Green and Zhang, 2013; Kueh et al., 2019). For the default flux option (referred to here as sf0), the momentum roughness length is given as in Charnock (1955) the momentum roughness length is given as Charnock's (1955) expression plus a viscous term, following Smith (1988) - Eq. (1):

$$z_o = \alpha \left(\frac{u^2}{g} \right) + \frac{0.11v}{u} \; , \tag{1}$$

where α is the Charnock coefficient and v the kinematic viscosity of dry air, for which a constant value of 1.5×10^{-5} m2 s^{-1}

210 is used. A constant value of α=0.0185 is used for sf0.

Since the roughness length formulas in sf0 are demonstrably inconsistent with a substantial amount of research (Kueh et al. 2019), two more options were developed (hereinafter referred to as sf1 and sf2) (Kueh et al. 2019). Based on the findings that the drag coefficient (CD) seemed to level off at hurricane force wind speed (e.g., Powell et al., 2003; Donelan et al., 2004),

215 the surface flux option 1 (sf1) was developed and implemented in WRF as a blend of two roughness length formulas (Green and Zhang 2013). The sf1 option was first implemented in version 3.0 of WRF (Kueh et al. 2019). The sf1 and surface flux option 2 (sf2) has the same momentum roughness length, but in sf2, the temperatures and moisture roughness lengths are expressed in accordance with Brutsaert (1975) (MMML-NCAR, 2019).

220 A set of experiments is conducted to explore the impacts of nudging on the ERA5 large-scale environment by applying spectral nudging (snON). It has been shown that spectral nudging can improve TC track simulations (Guo 2017; Tang et al., 2017) by constraining the model to large scale environmental conditions (Gilsan et al., 2013). Present-day simulations typically use nudging to reduce the mean biases in a relatively large domain (e.g., Xu and Yang 2015; Liu et al., 2016; Shen et al., 2017; Moon et al., 2018). Another set of experiments were also conducted without applying this technique (snOFF). Based on the

225 methodology of Moon et al. (2018), the spectral nudging for the horizontal and vertical wind components, the potential temperature, and the geopotential height was applied. The nudging coefficients for all variables were set at 0.0003 s^{-1}, applied at all levels above the PBL.

To assess the model sensitivity to various physics parameterizations and other model choices, we have systematically altered the choice of cumulus schemes and surface flux options. The use of spectral nudging is also explored in a set of experiments.

230 Table 2 shows the set of different model configurations.

Table 2: Summary of the sensitivity experiments with the parameterizations used

Cumulus scheme	Nudging	Surface flux option (isftcflx)*		
		isftcflx = 0 (sf0)	*isftcflx* = 1 (sf1)	*isftcflx* = 2 (sf2)
KF (KF)	Without spectral nudging (snOFF)	KFsnOFFsf0	KFsnOFFsf1	KFsnOFFsf2
	With spectral nudging (snON)	KFsnONsf0	KFsnONsf1	KFsnONsf2
TK (TK)	Without spectral nudging (snOFF)	TKsnOFFsf0	TKsnOFFsf1	TKsnOFFsf2
	With spectral nudging (snON)	TKsnONsf0	TKsnONsf1	TKsnONsf2

The control simulation is the experiment with KF as cumulus scheme, with spectral nudging turned off and surface flux option

235 of sf0 (KFsnOFFsf0). This configuration was also used in the experiments using the different members of EDA, to test the sensitivity to different initializations.

Other parameterization schemes (adapted from Li et al., 2018) in the model that remained the same in all the experiments, includes: the Rapid Radiative Transfer Model (RRTM) scheme (Mlawer et al., 1997) and the Dudhia scheme (Dudhia 1989)

240 for the longwave and shortwave radiation, respectively; surface layer is from the MM5 Monin- Obukov scheme (Monin and Obukhov 1954); WRF Single–moment 6–class Scheme for the cloud microphysics (Hong and Lim 2006); and Yonsei University (YSU) PBL scheme (Hong et al., 2006); and the Unified Noah Land Surface Model (Chen and Dudhia 2001; Tewari et al. 2004) for the land surface processes and structure.

245 **2.5 Verification Data**

To determine the model's skill in simulating TY Haiyan, we used the International Best Track Archive for Climate Stewardship (IBTrACS) which compiles best-track information from various agencies worldwide (Knapp et al., 2010). We compared the simulated and observed tracks by calculating the Direct Positional Error (DPE). Heming (2017) defines DPE as a measure of the great circle distance between observed and forecast positions at the same simulation time. We calculated the model bias,

250 root-mean-square error (RMSE), and correlation coefficient between model-simulated and observed (IBTrACS) minimum sea level pressure, maximum 10m winds, and IBTrACS to evaluate simulated TC intensity. The best-track information used here is taken from the World Meteorological Organization (WMO) subset of the IBTrACS (IBTrACS-WMO, v03r09) which was taken from the best-track data provided by the Japan Meteorological Agency (JMA). In order to directly compare the IBTrACS / JMA data with WRF's simulated winds, the 10-min averaged winds from the JMA dataset were converted to 1-min wind

255 speeds using Li et al.'s (2018) formula i.e. multiplying the 10-min values by 1.1364.

In addition, rainfall data from the Global Precipitation Measurement (GPM) is also used for comparing the spatial distribution of the simulated rainfall. The Integrated Multi-satellitE Retrievals for GPM (IMERG) is a third-level precipitation product of GPM, which covers the area -180, -90, 180, 90 with resolutions of 0.1 degree and 30 minutes (Huffman et al. (2019). The

260   rainfall data were accessed and downloaded from NASA's Goddard Earth Sciences Data and Information Services Center
(GES DISC) at https://disc.gsfc.nasa.gov/datasets/.

2.6 TC Tracking Method

The simulated track and intensity values were obtained every 6 hours using the TRACK algorithm (Hodges et al., 2017) as

265   used in Hodges and Klingaman (2019). TRACK determines TCs as follows: first the vertical average of the relative vorticity
at 850-, 700-, and 600-hPa levels is obtained. The field is then spatially filtered using 2D discrete cosine transforms equivalent
to T63 spectral resolution and the large-scale background is removed. The tracking is performed by first identifying the
vorticity maxima $> 5.0 \times 10^{-6}$ s^{-1}. Using a nearest neighbour method, the tracks are then initialized and refined by minimizing
a cost function for track smoothness subject to adaptive constraints (Villafuerte et al., 2021). The feature points are determined

270   by first finding the grid point maxima which are then used as starting points for a B-spline interpolation and steepest ascent
maximization method, to determine as the off-grid feature points (Hodges 1995 as cited by Hodges and Klingaman, 2019).
The tracking is done for the entire simulation period. Additional variables are added to the track data after the tracking is
complete, such as the maximum 10-m winds within a 6^0 geodesic radius and the minimum sea level pressure (MSLP) within
a 5^0 radius using the B-splines and minimization method (Hodges and Klingaman, 2019).

275   **3. Results and Discussion**

3.1 Simulated track

Fig. 2 shows the tracks obtained from the simulations of TY Haiyan for all experiments are in reasonably good correspondence
with the best-track data. Simulations using the TK scheme accurately reproduced the observed positions of TY Haiyan during
the first 36 h of the study period, with the observed and simulated tracks being less than 50 km apart at 36 h. On the other

280   hand, the simulated tracks based on the KF cumulus convective scheme tracked in the same direction as the observed track,
but were further north and more than 50 km from the best track during the first 36 hours of simulation.
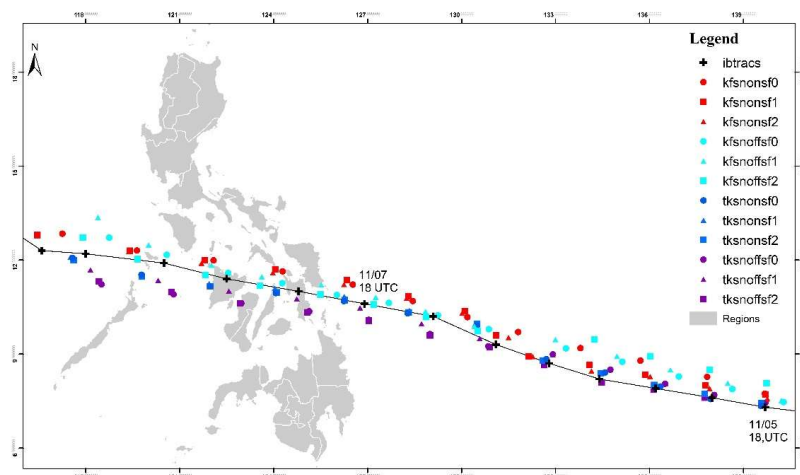
285   **Figure 2: Simulated tracks compared with IBTRaCS and the sensitivity experiments classified according to experiment groups: Kain-Fristch (KF) convection scheme; TK (TK) convection scheme; with spectral nudging (snON); w nudging (snOFF); surface flux option 0 (sf0); option 1(sf1); and option 2 (sf2).**

Fig. 3 shows the DPE throughout the simulation and shows the KF simulations having a mean DPE of 94 km while the TK

290   simulations having a mean of 62 km DPE. The simulations with the KF scheme have tracks that are further north of the

observed track compared to simulations utilizing the TK scheme which are closer to the observed track. The minimum DPE

obtained from the simulations using the TK scheme is 8km after 18 hours of simulation for the simulation using TKsnOFFsf2.

Fig. 3 shows the sensitivity of the tracks to the cumulus parameterization scheme, surface flux options, and to spectral nudging.

295   The results show that these three model settings individually lead to significant reductions in DPE values. The difference

between the mean DPE of simulations using KF and TK schemes (p-value: 0.010) were found to be statistically significant at

99% confidence levels using a Student's t test. The simulations using the TK scheme have mean DPE of 47 ± 5 km and KF

scheme have mean DPE of 55 ± 7 km (Fig. 3a). Overall, we found the TK scheme to be best in simulating the track of TY

Haiyan.

300

Our results show that the tracks are also slightly sensitive to the use of spectral nudging, especially in the latter half of the

simulation (Fig. 3b). The evolution of DPE in Fig. 3 shows gradual increases in its value in the first half of the simulation, as

the typhoon approaches land (between 48 h-54 h), the DPE then starts to abruptly increase until the end of the simulations.

This suggests that the spectral nudging configuration does not constrain the model strongly. Nevertheless, simulations run with

305   spectral nudging consistently show lower DPE in the 2nd half of the simulation compared to the no nudging experiments.

Moreover, the TK runs appear to also have less dependence on nudging (not shown). The mean DPE of the TK simulations

with nudging is 68 km while the simulation without nudging is 87 km. This is consistent with previous studies where spectral

nudging improves TC tracks in the WNP (Guo 2017; Moon et al., 2018). Overall, the surface flux options did not have a

significant effect on the tracks of the simulated TY (Fig. 3c).

310
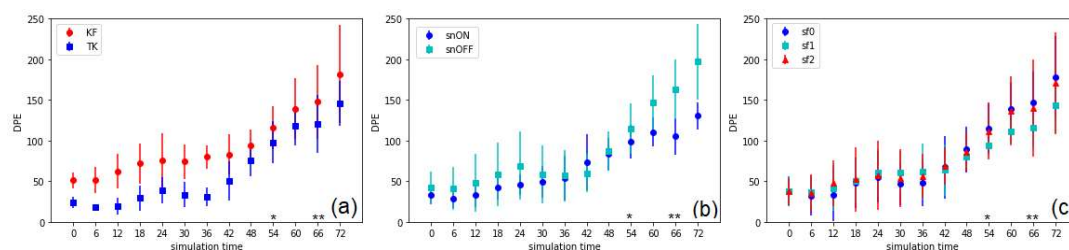
Figure 3: Mean and standard deviation of the DPE per simulation group – (a) for the cumulus schemes KF and TK, (b) for with (snON) and without nudging (snOFF) and (c) for surface flux options sf0, sf1 and sf2. The one and two black stars along the x-axis of the DPE (inset) show the approximate average time the simulated TC entered and exited land, respectively.

315

3.2 Simulated intensity

Fig. 4 shows that most of the simulations are not able to capture the observed deepening of the minimum central pressure or

the intensification of low-level winds of TY Haiyan. The control simulation (denoted as KFsnOFFsf0) has a MSLP value of

only 934 hPa and maximum wind speed of 53.69 meters per second (ms^{-1}). Compared to the minimum central pressure of

320   895hPa and 73 ms^{-1}1-min sustained wind speed in the observations, this is a difference of 39 hPa and 19 ms^{-1}, respectively.

The simulations that are closest to TY Haiyan's intensity are those that use the KF scheme and surface flux option 1

(KFsnONsf1), however, this simulates lower than observed MSLP value at the first 12 hours of simulation. The KFsnONsf1

run has a MSLP reaching to 912 hPa and winds of up to 72 ms^{-1}. The TK scheme simulations consistently have higher central

pressure and lower maximum wind speeds. A Student's t test indicates that difference between the minimum sea level pressure

325   simulations using KF and TK schemes (p-value: 0.008) is significant at the 99% confidence level. However, the simulations

were not able to capture TY Haiyan's rapid intensification phase as in previous studies (Islam et al., 2015; Kueh et al., 2018).
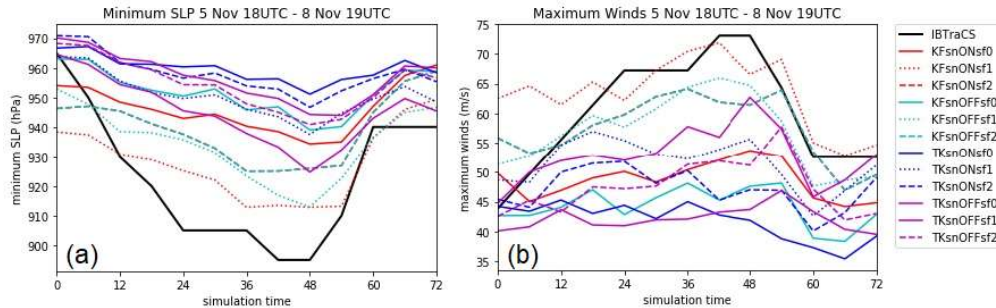
Figure 4: Time series of intensity (a) for minimum sea level pressure in hPa and (b)for the sensitivity experiments classified according to experiment groups: Kain-Fristch (KF) convection scheme; TK (TK) convection scheme; with spectral nudging (snON); without spectral nudging (snOFF); surface flux option 0 (sf0); option 1(sf1); and option 2 (sf2)

Fig. 5 shows the mean and standard deviation of the biases of the simulated intensities to the choice of the parameterization

335   schemes. There is a significant difference among the simulations using KF and TK cumulus convection schemes (Fig.5, 1st

row). In simulating the intensity, nudging did not demonstrate a consistent improvement in the intensity of the simulations

(Fig. 5, 2nd row). While the choice of surface flux option had a more demonstrable effect on the resulting intensities (at 99%

confidence levels) with sf1 having the most intense simulation of the storm in terms of both MSLP and maximum winds and

sf0 with least intensity (Fig. 5,3rd row).

340
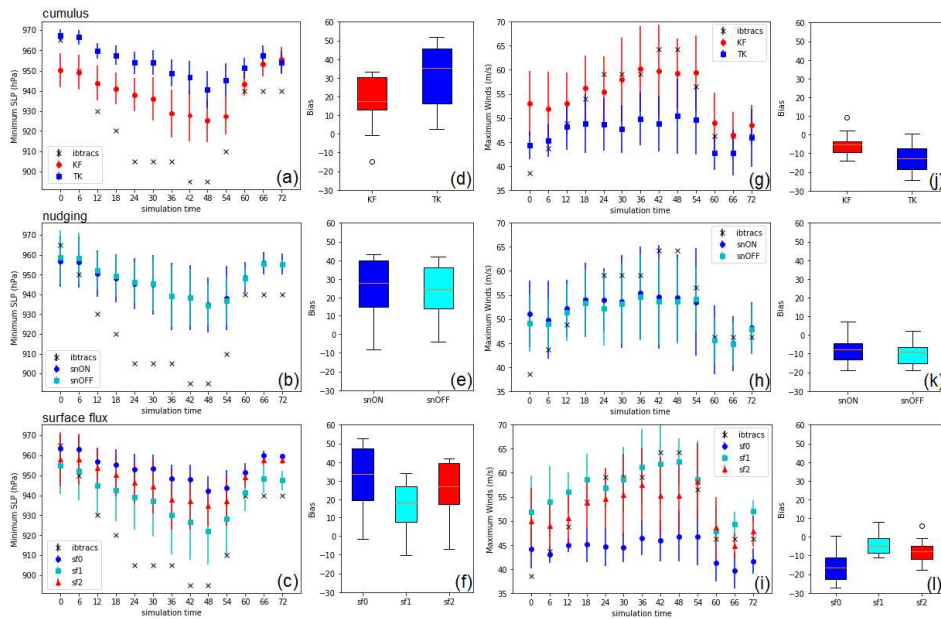
Figure 5: Time series of the mean intensities and standard deviations (a-c) for MSLP and (g-i) for maximum winds, with mean biases for MSLP (d-f), hPa and maximum winds, m/s for each group (j-l) for cumulus schemes KF and TK, spectral nudging and for surface flux options.

345

Fig. 6 shows that the simulations using the KF scheme have higher correlations and smaller RMSE values than the simulations that used the TK scheme. The simulations with the KF scheme are comparatively more successful at simulating the intensity for both minimum surface pressure and maximum winds. Of all the simulations, the simulation with the combination of KF and sf1 without nudging have the lowest RMSE (22 hPa MSLP and 6 ms^{-1} maximum winds) and highest correlation coefficient

350 of 0.78 and 0.89 for MSLP and maximum winds, respectively. While the simulation with the poorest performance i.e. highest RMSE (37 hPa and 20 ms^{-1}) and lowest correlation coefficient (0.60 and 0.21 for MSLP and maximum winds, respectively) is the simulation with the combination of TK, sf0, with spectral nudging turned on.

The KF and TK schemes represent shallow convection differently, resulting in different simulated TC intensities (Torn and

355 Davis, 2017). The TK scheme allows both upward transport of moisture across the boundary layer, as well as vertical advection of evaporation from the ocean surface (Parker et al., 2018). Consequently, this reduces the mass flux in deep convection, thereby lowering the rate of TC intensification and resulting in lower simulated intensities. The KF scheme, however, is less likely to reduce the deep convective mass flux that allows for intensification rates to increase. These results are consistent with the differences in the simulated intensities shown in Parker et al. (2017) and Shepherd and Walsh (2016). Parker et al. (2017)

360 found that the KF scheme produces more intense TC systems (lower MSLP values) than the TK scheme for TY Yasi in Australia. Shepherd and Walsh (2016) also found that the KF scheme produces stronger storms (TY Yasi 2011 in the Southwest Pacific and TY Rita 2005 in the north Atlantic) but almost the same intensity for simulations using TK and KF schemes for TY Megi in the Western North Pacific Basin.

365
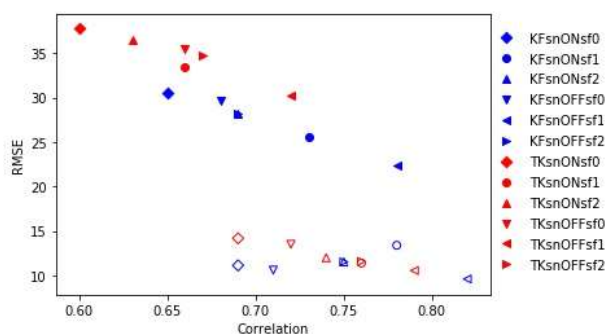
Figure 6: RMSE vs CC for minimum sea level pressure in hPa (filled) and for maximum winds in ms-1 (not filled) for the sensitivity experiments

The choice of surface flux option (sf0, sf1, sf2) also affects the ability to reproduce both minimum sea level pressure and

370 maximum winds, as shown by the lower RMSE of sf1 (Fig. 6). Simulations with sf1 have generally shown to have the highest correlation coefficients. While both wind speed and MSLP intensity are strongly dependent on the surface flux option, sf1 shows to simulate the highest intensity for TY Haiyan. As in Kueh et al. (2019), the default option (sf0), in which CD does not level off, the simulation of Haiyan has the weakest wind speeds. The sf1 option is expected to have the highest intensity since it has the largest enthalpy and momentum (Ck/CD) ratio at high wind speeds and lowest CD. This gives less friction at high

375 winds, thereby favouring higher intensity (Kueh et al. 2019).

Natural Hazards
and Earth System
Sciences

Open Access

Discussions

EGU

Comparing the simulations with the KF and TK schemes shows that the former produces better simulated intensities with lower biases, RMSE and higher correlation coefficients (Fig. 6), consistent with Zhang et al. (2011) and Parker et al. (2017), and minimum sea level pressure as with Spencer and Shaw (2012).

380

Table 3: The resulting deviation from landfall location (km, rounded to nearest whole number); translation speed (ms⁻¹, rounded to two decimal place); and deviation from observed translation speed (ms⁻¹, rounded to two decimal places); and deviation of the simulated MSLP at landfall (hPa, rounded to the nearest whole number); compared to observations

Simulation	Deviation from landfall point 10.83°N, 125.69°E (in km)	Translation speed before landfall (ms⁻¹) (Obs. 9.48 ms⁻¹)	Deviation from observed translation speed before landfall	Deviation from observed MSLP (895 hPa) at landfall
KFsnONsf0	56	9.62	0.14	40
KFsnONsf1	76	8.78	-0.70	18
KFsnONsf2	55	8.76	-0.72	32
KFsnOFFsf0	20	9.27	-0.22	46
KFsnOFFsf1	37	9.54	0.05	27
KfsnOFFsf2	3	9.58	0.10	44
TKsnONsf0	6	9.80	0.32	56
TKsnONsf1	11	9.87	0.39	43
TKsnONsf2	3	9.85	0.37	52
TKsnOFFsf0	56	9.23	-0.25	49
TKsnOFFf1	68	9.54	0.06	38
TKsnOFFsf2	61	9.20	-0.29	48

385 We also considered the wind-pressure relationship of the simulated intensities of all experiments, which according to Green and Zhang (2013) is affected by surface flux options. The scatterplot in Fig. 7 indicates the relationship between the MSLP and maximum wind, based on the different simulations. The IBTrACS data (black square markers) are also included in this plot. Almost all simulations show a decreasing trend of the MSLP and maximum winds as the storm intensifies; however, the intensities are evidently underestimated (MSLP and maximum wind speeds). Based on Manganello et al. (2012), the maximum

390 wind speed is usually underestimated in RCMs when the simulated MSLP is below approximately 980 hPa. It is worth pointing out that of the different simulations, those utilizing the surface flux option 1 (sf1, blue) give the most intense storm by wind speed (Fig. 8). The simulated maximum wind speeds in the simulations using the default surface flux option (sf0, red) only ranges between 35 to 55 ms⁻¹ while the simulations using the other options (sf1, blue and sf2, cyan) are well distributed from ~40 to 73 ms⁻¹, consistent with the result of Kueh et al. (2019). Most simulations have an underestimated maximum wind

395 speeds for MSLP below 910 hPa, which is consistent with a study using WRF that produced lower wind speed compared to IBTrACS for a given MSLP (Hashimoto et al., 2015). However, the simulations were able to generate considerable intensity for the maximum wind speed for TY Haiyan compared to that of Islam et al. (2015) who used different model physics options i.e. WRF single moment 6-class (WSM6), WRF single moment 3-class (WSM3), new Thompson (THOM), Milbrandt-Yau double moment (MY2) 7-class scheme, and the Goddard GCE (GGCE) schemes. Previous studies using lower resolution

400 generated insufficient wind speeds in the regime higher than 45 ms⁻¹ (Jin et al., 2015) which are primarily attributed to low model resolutions and deficiencies in surface drag representations at high wind conditions (Jin et al., 2015; Shen et al., 2017).
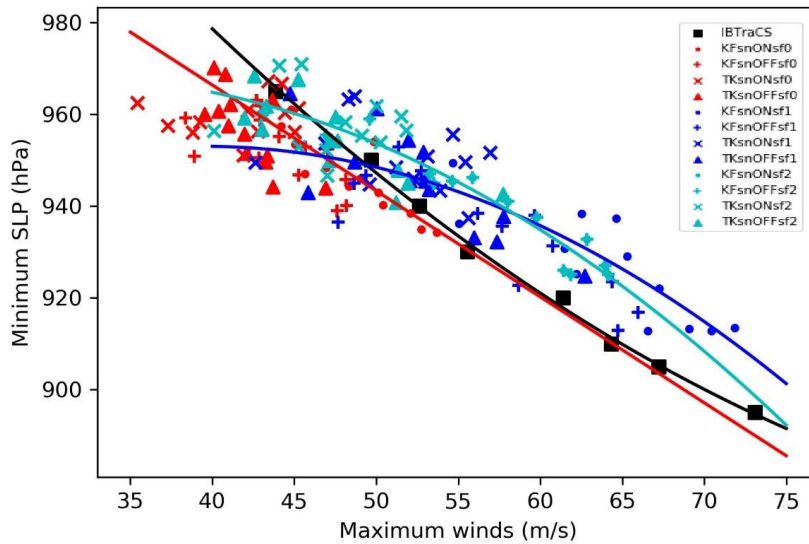
Figure 7: Scatterplot of MSLP vs maximum wind from the various sensitivity experiments compared with best track data. Solid lines of the corresponding colours (red for sf0, blue for sf1, cyan for sf2) show the second-order polynomial fit.

In simulating TCs, it is important to get the timing and intensity at landfall right as it gives a good indication of the potential damage along coastal areas (Parker et al. 2017). TY Haiyan made landfall in the eastern-central Philippines (Guiuan, Eastern Samar) on 7 Nov 2013 at 2040 UTC. Table 3 shows that the simulation with the closest landfall time and location occurs for the KFsnoffsf2 simulation. The deviation from the observed landfall point, minimum deviation is 3 km for KfsnOFFsf2 and TKsnONsf2 and maximum deviation is 76 km for KFsnONsf1, is within the average forecast error for tropical cyclones at 24-hour lead time in Western North Pacific (Peng et al, 2017).

Fig. 8 also shows that the simulated TY is slightly slower (farther from land on 7 Nov 2013 at 00UTC) than observed, with the timing of landfall delayed between approximately 2 to 6 hours in the simulations. Based on data from IBTrACS, Haiyan's translation speed before landfall is approximately 9.48 ms^{-1}, while the mean translation speed of all the simulations is 9.43 ms^{-1} as shown in Table 3. Fig. 8 also shows that the extent of the wind field of the simulations using KF scheme are wider than the ones using TK scheme. The KF scheme simulations have a bigger radial extent, for winds speeds larger than 35 ms^{-1} or 80 miles per hour (mh^{-1}), than the simulations using the TK scheme. The wind field extent is also bigger in simulations with sf1 and sf2 than the ones using the default surface flux option (sf0), with sf1 having a wider and more symmetric radial extent of winds greater than 50 ms^{-1} or 110 mh^{-1}. TY Haiyan's radius of maximum wind was estimated to be between 25-29 km (Shimada et al, 2018). In addition, the radial extent of winds of approximately 15 ms^{-1} (30 mh^{-1}) is bigger in simulations using KF than simulations using TK scheme, with radius of maximum wind extending up to ~52 km and ~42 km, respectively. The TKsnONsf0 and TKsnOFFsf0 both have radial extent of winds of 15 ms^{-1} (30 mh^{-1}) that are closer to what is estimated using the OSCAT scatterometer data.

3.3 Simulated Track and Intensity from ERA5 EDA Ensemble Members

The simulated tracks of TY Haiyan, using the four ERA5 EDA members as initial and boundary conditions and configurations that are the same as used for the control simulation, are found to be within the variability of the simulations using the different

parameterizations (Fig. 9). The average DPE of the ensemble mean is 86 km compared to the average DPE of the simulations using different parameterizations which is 78 km with a range from 7 km to 250 km throughout the whole simulation period. There is no significant difference between the mean DPE of the simulations using the different ensemble members with the simulations using the different parameterization schemes (p-value = 0.464).
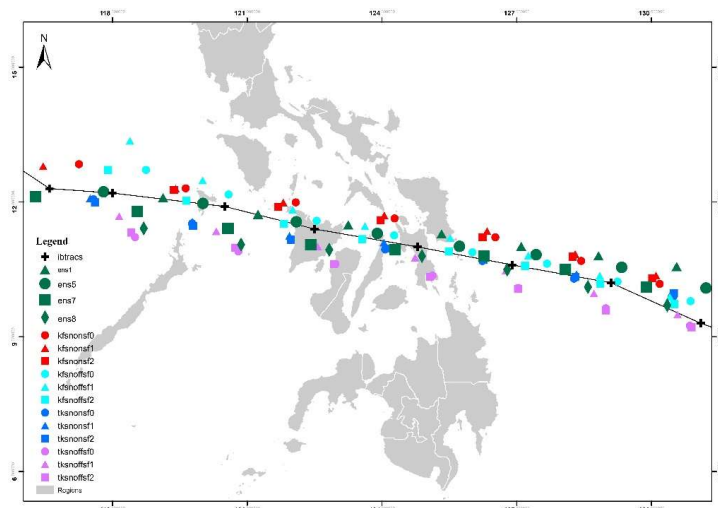
435
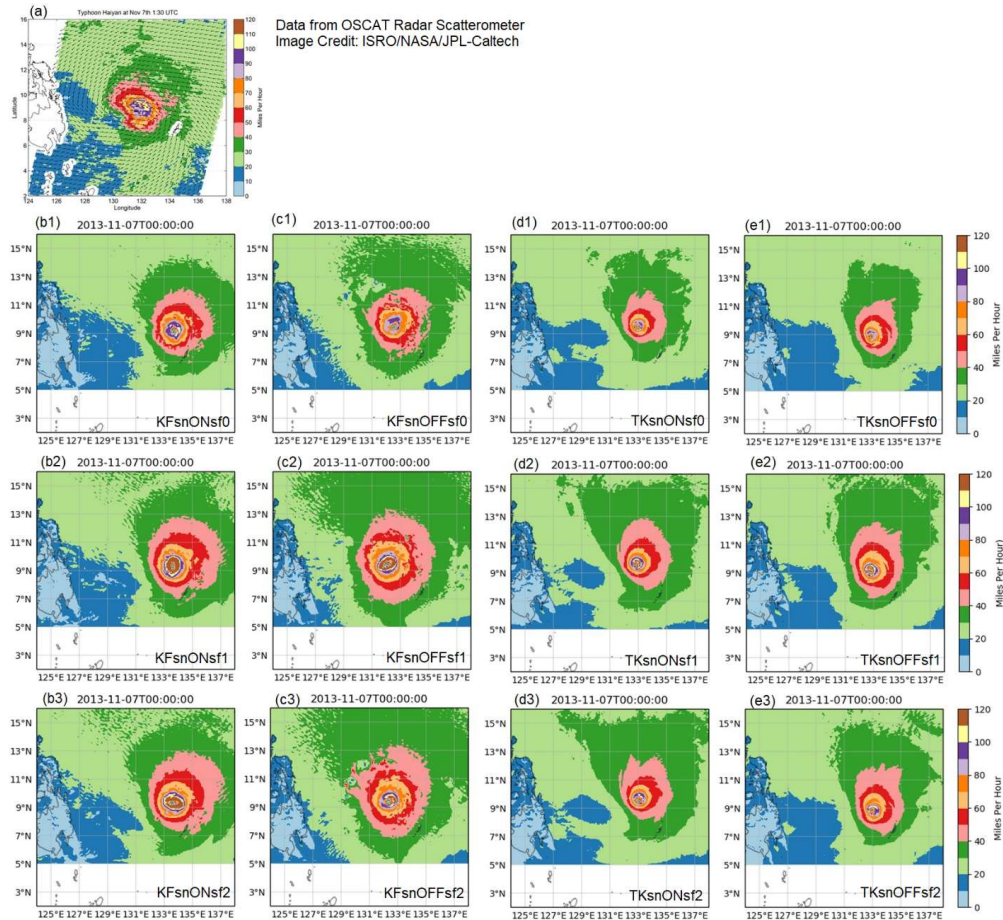
Figure 8: Surface winds (mh⁻¹) (a) from the OSCAT radar scatterometer on the Indian Space Research Organization's OceanSAT-2 satellite at 0130UTC 7 November 2013[1] and (b-e) for each of the experiments at 00 UTC 7 November 2013.

440

---

[1] *Source of Figure 8a: https://www.jpl.nasa.gov/images/super-typhoon-haiyan. Use is covered by https://www.jpl.nasa.gov/jpl-image-use-policy*

Figure 9: Simulated tracks of the four randomly selected EDA Ensemble Members (green) compared with IBTRaCS and the sensitivity experiments classified according to experiment groups: Kain-Fristch (KF) convection scheme; TK (TK) convection scheme; with spectral nudging (snON); w nudging (snOFF); surface flux option 0 (sf0); option 1(sf1); and option 2 (sf2).

The spread in the mean bias of the simulated intensities (MSLP and maximum winds) using the ensemble members as boundary conditions is similar to or within the spread of the correlation between the experiments with the different parameterization schemes and spectral nudging option (Fig. 10). Judging from the spread of the simulate intensities found in the boundary conditions experiments, the use of different ensemble members has relatively less effect on the simulated intensities as compared to the sensitivity to cumulus and surface flux parameterizations.
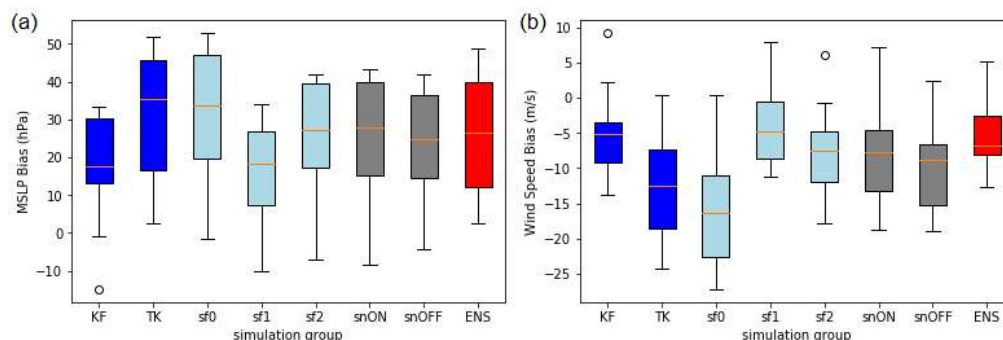
Figure 10: Mean biases for (a) MSLP in hPa and (b) maximum winds in ms-1 for each group of simulations: cumulus schemes KF and TK (blue bars), surface flux options (sf0, sf1, sf2) (light blue bars), spectral nudging ON and OFF (gray bars), and mean of the different experiments using four randomly selected EDA ensemble members (ENS) (red bars) as initial and boundary conditions.

3.4 Simulated Rainfall

The simulated rainfall in WRF is represented implicitly to demonstrate the effects of sub-grid scale processes through the cumulus scheme and explicitly through the microphysics scheme. In this study, we used the combination of both implicit and

explicit precipitation as the total rainfall. The spatial distribution of rainfall (mm) from 00 UTC 7 November 2013 to 18 UTC

8 November 2013 from the different experiments without spectral nudging are presented in Fig. 11. These results show a

465   discernible difference between the spatial distribution and magnitude of the simulated rainfall, which indicates high sensitivity

to the cumulus schemes. The accumulated 6-hourly rainfall was generally larger in magnitude and spatial extent for the

simulations using the KF scheme (Fig. 9 b-d) than those that used TK scheme (Fig. 9 e-g). There is not much difference in the

magnitude and distribution of rain among the different surface flux options.

470   It is also important to note the delay in the rainfall at landfall, primarily due to the relatively slower movement of the simulated

TCs. The extent of the distribution of rainfall outside of Haiyan's inner rain bands were also not captured well by the

simulations when compared with the satellite-derived GPM rainfall (Fig. 11a). In comparison with the GPM rainfall, the

distribution of the simulated high rainfall using the KF scheme show more similar patterns unlike with the TK scheme. The

areas of high rainfall appear to be similar in the simulations using different flux options but different in simulations using KF

475   and TK scheme. The simulations using KF scheme also seem to capture the outer rainbands of TY Haiyan, but extending

further southeast compared to the GPM rainfall. Previous studies have also indicated the sensitivity of TC-associated rainfall

to different physics parameterizations in WRF. Satuya et al. (2019) and Duc et al. (2019) found that KF better predicts rainfall

than TK but both generally perform poorly in simulating rainfall, and WRF TC-associated rain are underestimated (Bagtasa

2021).

480
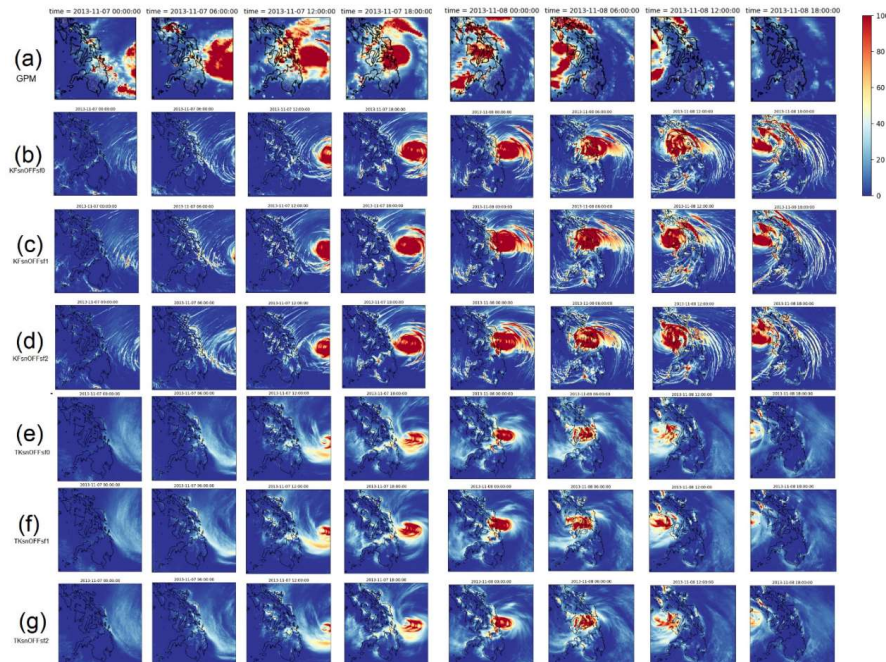
Figure 11: Spatial patterns of rainfall (in mm) every 6-hours from 00 UTC 7 Nov 2013 to 18 UTC 8 Nov 2013 (a) GPM, and the different simulations without nudging using (b,c,d) KF with sf0, s1,sf2 respectively, and (e,f,g) TK with sf0, sf1, sf2 respectively.

485

Natural Hazards
and Earth System
Sciences
Discussions

3.5 Environmental Factors

Based on previous similar studies (Parker et al. 2017; Torn and Davis 2012) and as shown in Fig. 12, the KF scheme results in a warm temperature bias (at 700hPa) and a steering flow bias (at 850 hPa). In particular, the TK scheme produces cooler temperatures and the KF scheme simulates up to approximately 1.5 to 2°C warmer temperatures relative to ERA5, while the ones using the TK scheme have a colder bias at 700hPa (Fig. 12), which is consistent with previous studies (Parker et al. 2017 and Shepherd and Walsh 2016). On the other hand, the KF scheme is likely to simulate the deep convective mass flux which allows for an increase in intensification rates (Zhu and Smith 2002; Emanuel 1989 as cited by Torn and Davis 2012).
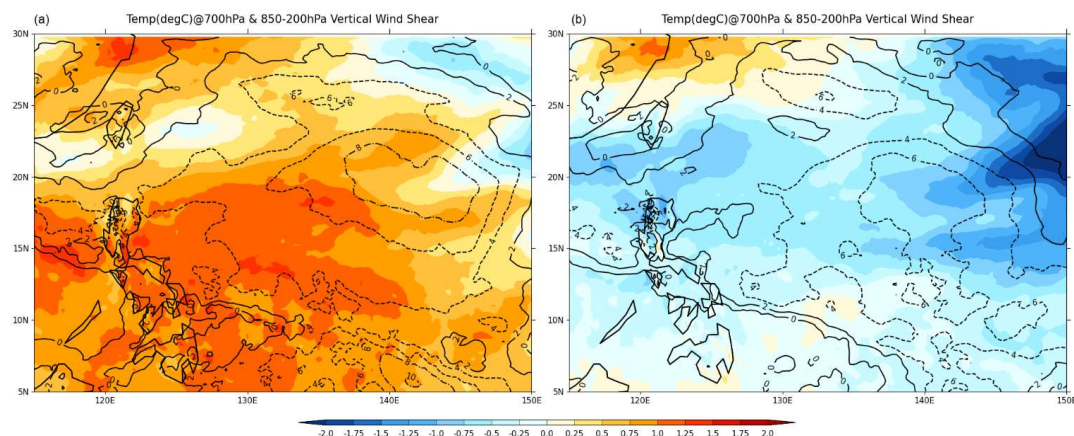
Figure 12: The difference of the simulated temperature (in degree Celsius) at 700hPa (contour) and deep vertical wind shear averaged over the entire period of the simulation with (a) KF (corresponding to kfsnoffsd1) and (b) TK (corresponding to tksnoffsd1) temperature and winds from ERA5

Fig. 12 also displays the simulated deep layer vertical wind shear (contour), which is defined as

$$Vertical\ Wind\ Shear = \sqrt{(U200 - U850)^2 + (V200 - V850)^2},$$ (2)

where u, v are the zonal and meridional wind components, respectively, at 200 and 850 hPa. The simulated vertical wind shear is weaker along the track of TY Haiyan for both simulations using KF and TK, but the simulation using KF has a bigger area with weaker shear. It is likely that the more homogeneous temperature field in KF resulted in less vertical wind shear, while the simulation using the TK scheme led to a more heterogeneous temperature increasing the vertical shear. A previous study by Floors et al (2011) showed that the temperature differences through the atmospheric profile leads to geostrophic wind shear in WRF simulations. With the weaker vertical shear, the intensity is higher in the simulation using KF than the simulation using TK scheme. Weaker vertical shear has been found to be favourable in maintaining TC development and intensity (Shen et al., 2019).

To further investigate the difference in the track between KF and TK simulation runs, we analysed the 500mb geopotential height. The 5800 m geopotential height contour at 500 mb is used to depict the western North Pacific sub-tropical high (WNPSH) (Xue and Fan 2016). With the ridge location at 20°E, the WNPSH extends to the north of South China Sea (Shen et al., 2019). It has been found that the westward extent and location of the subtropical high ridge directly affect TC tracks in the WNP basin (Ho et al., 2004). In the simulation using the KF scheme, the subtropical high is weaker and is substantially in a more northward position compared to the simulation using the TK scheme (Fig. 13), which likely causes the tracks of the

simulations using the KF scheme to drift northward, while the simulations using the TK scheme are much closer to the observed. According to Sun et al. (2014), deep convection in mass flux schemes, such as KF, produces large amounts of anvil

520   clouds that warm the upper troposphere and cause latent heating south of the WNPSH that leads to the weakening of the WNPSH and the movement of the TCs northward. Villafuerte et al. (2021) further added that the use of cumulus schemes results in a weaker subtropical high resulting in shifts in northward re-curvature of TC tracks.
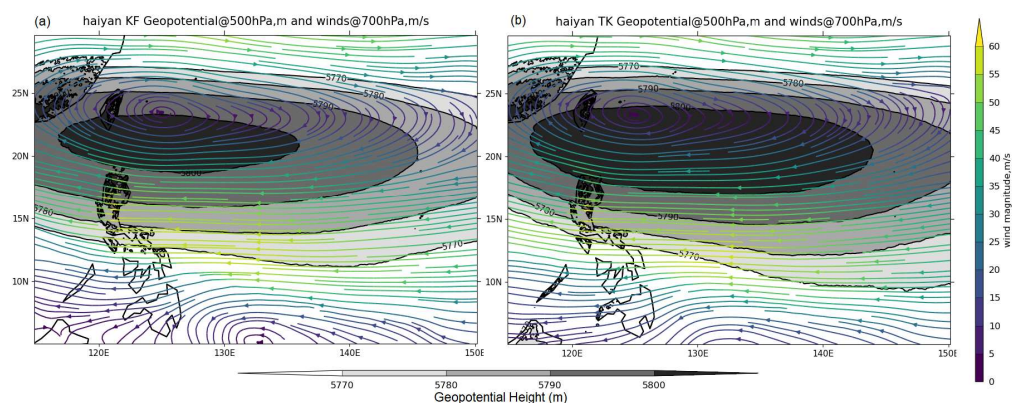

525

Figure 13: Geopotential height at 500hPa in geopotential meters shaded contour lines and winds (streamlines) at 700hPa averaged over the entire period of the simulation with (a) KF (corresponding to kfsnoffsd1) and (b) TK (corresponding to tksnoffsd1)

The TK scheme also produced relatively drier storm environments along the TC path compared to the simulation using KF

530   scheme and as a result, less convection, which translates into weaker intensity (lower wind speeds), whereas simulations using the KF scheme are ~15% higher relative to the simulation using TK. The TK scheme has relatively drier bias with respect to ERA5 along the TC track (Fig. 14). According to Villafuerte et al. (2021), the TK scheme underestimates mid-tropospheric relative humidity, providing a drier environment thereby constraining deep convection and inhibiting TC development. Furthermore, Shen et al. (2019) demonstrated that drier lower troposphere enhances downdrafts and inhibit convection,

535   resulting in weaker intensities and less rain. When comparing the distribution of mid-tropospheric relative humidity as shown in Fig. 14, KF shows a lower relative humidity along the track of Haiyan, which indicates better vapor to precipitation conversion of the KF scheme. From this distribution of relative humidity, it can be easily assumed that the KF scheme produces more convection and generated significant rainfall associated with the system, as compared to the weaker convective organization (hence less rainfall) of the simulations using the TK scheme.

540
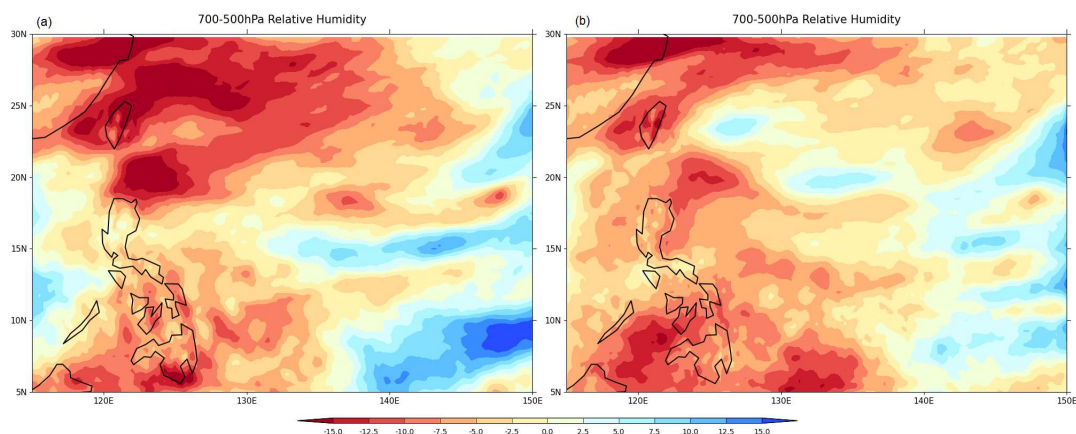
Figure 14: The difference of the simulated Mid-tropospheric (700-500hPa) Relative Humidity averaged over the entire period of the simulation with (a) KF (corresponding to kfsnoffsd1) and (b) TK (corresponding to tksnoffsd1) from ERA5

4. Conclusion

545

Typhoon Haiyan (2013) was one of the most intense and destructive tropical cyclones ever to hit the Philippines. As climate models project more intense storms, such as Typhoon Haiyan, will occur more frequently in the future due to climate change, it is important to improve their representation in high-resolution models, in order to improve understanding of TCs under climate change and improve confidence in model projections, and more importantly, for risk and impact assessments. The

550 intensity of TY Haiyan proved difficult to simulate using the Weather Research and Forecasting model at 25-km and 5-km domain configurations as with other previous studies. This study was able to assess the sensitivities to different parameterizations in WRF that can be useful in future simulations of TC cases under future climate conditions. Despite the failure to simulate Haiyan's rapid intensification phase, the simulations were still able to capture the tracks and intensity reasonably well. Based on the results, there seems to be a trade-off between utilizing KF and TK cumulus schemes that has

555 not been previously discussed in previous studies of tropical cyclones in the Philippines.

The simulated intensity of TY Haiyan is most sensitive to changes in the cumulus scheme and surface flux options; on the other hand, simulated track is most sensitive to cumulus scheme and spectral nudging. However, the TK cumulus scheme produces better track and the KF scheme produces better intensity. There is a statistically significant difference in the simulated

560 tracks and intensities between the use of the two cumulus schemes. The TK scheme simulates the track better, while the KF scheme produces higher intensities, with the KF scheme simulating a mean bias of 16 hPa and 2 ms^{-1} and the TK scheme with a mean bias of 31 hPa and -6 ms^{-1}, respectively. The KF scheme has larger DPEs (mean DPE of 94 km compared to mean DPE of 61 km for TK scheme) due to a more northward steering flow. On the other hand, simulations using the TK scheme had weaker wind and higher MSLP due to the suppression of deep convection by active shallow convection. Simulated rainfall

565 is also sensitive to the cumulus schemes, with simulations using TK having less and smaller rainfall extent than simulations using KF cumulus convection scheme.

The results also show the simulated tracks are sensitive to spectral nudging which results in a reduction in the mean DPE by 20 km. The intensity varies as well with different surface flux options, with surface flux option 1, where the momentum

570 roughness length is expressed using a combination of two roughness length formulas (Green and Zhang, 2013), in which the first is Charnock (1955) plus a constant viscous term and the second is the exponential expression from Davis et al. (2008)

with a viscous term (as cited by Kueh et al., 2019) simulating better intensities than the other two options (default surface flux option and surface flux option 2). The use of boundary conditions from different ensemble members also resulted in variations in the simulated tracks and intensities, but still within the range of variability of the different parameterization experiments.

575 The use of the KF convective scheme and a more reasonable surface flux option (sf1) can help improve the simulated intensity. While the use of the TK convective scheme and application of spectral nudging can improve the track simulation.

This study is part of an on-going effort to investigate the effect of future climate on the intensity and track of selected destructive TC case studies in the Philippines such as Haiyan using a regional climate model. The resulting sensitivities to the

580 cumulus schemes will be an important consideration in simulating the TC case studies with climate change forcing. Our findings further stress the need for choosing the appropriate cumulus schemes and surface flux parameterization given its impacts on different TC characteristics, e.g. the KF scheme and surface flux option 1 for simulating better intensities of extreme TCs such as Haiyan, besides higher grid resolutions as noted in previous studies (Kueh et al., 2019, Li et al., 2018). The results presented here can also be used in further improving the value of downscaling for simulating intense TCs like Haiyan. These

585 and future results will be useful in addressing the growing need to plan and prepare for, and reduce the impacts of future TCs in the Philippines. As shown in this study, there are uncertainties associated with the use of cumulus parameterizations schemes, spectral nudging and surface flux parameterizations. To cover these uncertainties, the use of ensemble simulations can be applied. For operational applications, an ensemble of cumulus parameterizations can be used to take into account the uncertainty in the track and intensity of simulation intense TCs. This study can facilitate research on regional climate modeling

590 to improve simulations of intense TCs like Haiyan. Furthermore, it is important to study RCMs with a model resolution less than 5 km that can be extremely useful in simulating TCs and associated rain. Li et al. (2018) suggested that a 2-km convection-permitting resolution is needed to reproduce intense TCs such as Haiyan. Other model parameterizations such as cloud microphysics and planetary boundary layer, and ocean coupling may help further improve the intensity simulations of extreme TC such as Haiyan but are beyond the scope of this paper. Simulations using a higher resolution convection-permitting model

595 is needed. Additional simulations and further investigations on these aspects, as well as for other similar TCs will be useful.

Appendices

none

Code availability

Code for the WRF model is available at http://www2.mmm.ucar.edu/wrf/users/downloads.html. WPS Geographical Input data
600 is available from https://www2.mmm.ucar.edu/wrf/users/download/get_sources_wps_geog.html#mandatory.
TRACK is available from https://gitlab.act.reading.ac.uk/track/track. CF-python and CF-plot were used in the analysis and visualization, and installation packages are available from https://ncas-cms.github.io/cf-python/

Data availability

Simulation data are stored at the JASMIN data storage facility and is available upon request from the corresponding author.

605 **Author contribution:**

RJD designed the experiments with guidance from GB, PLV and KH. RJD performed the simulations and analysis with inputs from all co-authors particularly the interpretation of the results. RJD wrote the article with contributions from all co-authors.

Natural Hazards
and Earth System
Sciences
Discussions

Competing interests:

The authors declare that they have no conflict of interest.

610 **Disclaimer**

none

References

Adeniyi, M.O.: Sensitivities of the Tiedtke and Kain-Fritsch Convection Schemes for RegCM4.5 over West Africa.
620 Meteorology Hydrology and Water Management. 7(2):27-37. doi:10.26491/mhwm/103797, 2019.

Aragon, L.G.B. and Pura, A.G.: Analysis of the displacement error of the WRF–ARW model in predicting tropical cyclone tracks over the Philippines. Met. Apps, 23: 401-408. doi:10.1002/met.1564, 2016.

625 Bagtasa, G.: Contribution of Tropical Cyclones to Rainfall in the Philippines. Journal of Climate. Vol 30. pp. 3621-3633. http://dx.doi.org/10.1175/JCLI-D-16-0150.1, 2017.

Bagtasa, G.: Analog forecasting of tropical cyclone rainfall in the Philippines. Weather and Climate Extremes,32, doi:10.1016/j.wace.2021.100323, 2021.
630

Biswas, M. K., Bernardet, L., and Dudhia, J.: Sensitivity of hurricane forecasts to cumulus parameterizations in the HWRF model, 9113–9119. doi:10.1002/2014GL062071, 2014.

Brucal, A., Roezer, V., Dookie, D. S., Byrnes, R., Ravago, M. V, and Cruz, F.: Disaster impacts and financing: local insights
635 from the Philippines, (June). https://www.lse.ac.uk/granthaminstitute/publication/disaster-impacts-and-financing-local-insights-from-the-philippines/, 2020.

Brutsaert, W.: A theory for local evaporation (or heat transfer) from rough and smooth surfaces at ground level, Water Resour. Res., 11, 543–550, doi:10.1029/WR011i004p00543, 1975a.
640

Brutsaert, W.: The Roughness Length for Water Vapor, Sensible Heat, and other Scalars, J. Atmos. Sci., 32, 2028–2031, doi:10.1175/1520-0469(1975)032<2029:TRLFWV>2.0.CO;2, 1975b.

Camargo, S. J., and Sobel, A. H.: Western North Pacific Tropical Cyclone Intensity and ENSO. J. Climate, 18, 2996–3006,
645   doi:10.1175/JCLI3457.1, 2005.

Cardenas, M.B., Bennett, P.C., Zamora, P.B., Befus, K.M., Rodolfo, R.S., Cabria, H.B., and Lapus, M.R.: Devastation of
aquifers from tsunami-like storm surge by Supertyphoon Haiyan. Geophys. Res. Lett. 42(8): 2844–2851,
doi:10.1002/2015GL063418, 2015.

650

Cayanan, E.O., Chen ,T-C., Argete, J.C., Yen, M-C., and Nilo, P.D.: The effect of tropical cyclones on southwest monsoon
rainfall in the Philippines. J. Meteorol. Soc. Jpn 89A:123–139, doi:10.2151/jmsj. 2011-A08, 2011.

Cha, E.J., Knutson, T., Lee, T., Ying, M. and Nakaegawa, T.: Third Assessment on Impacts of Climate Change on Tropical
655   Cyclones in the Typhoon Committee Region – Part II: Future Projections, Tropical Cyclone Research and Review, 2020,ISSN
2225-6032, doi:10.1016/j.tcrr.2020.04.005 , 2020.

Charnock, H.: Wind stress on a water surface, Q. J. Roy. Meteor. Soc., 81, 639–640, doi:10.1002/qj.49708135027, 1955.

660   Chen, F. and Dudhia, J.: Coupling an advanced land-surface/ hydrology model with the Penn State/NCAR MM5 modeling
system. Part I: model description and implementation. Mon Weather Rev 129:569–585, doi:10.1175/1520-
0493(2001)129<0569:CAALSH>2.0.CO;2, 2001.

Chen, S.H. and Sun, W.Y.: A one dimensional time-dependent cloud model. J Meteorol Soc Japan 80:99–118
665   doi:10.2151/jmsj.80.99, 2002.

Chen, J., Wang, Z., and Tam, C. Impacts of climate change on tropical cyclones and induced storm surges in the Pearl River
Delta region using pseudo-global-warming method. Sci Rep 10, 1965, doi:10.1038/s41598-020-58824-8, 2020.

670   Christensen et. Climate phenomena and their relevance for future regional climate change. In: Stocker et al., eds. Climate
Change 2013: The Physical Science Basis. Contribution of Working Group I to the Fifth Assessment Report of the
Intergovernmental Panel on Climate Change (IPCC AR5). Cambridge, UK and New York, NY: Cambridge University Press.

Cinco, T. A., de Guzman, R. G., Ortiz, A. M. D., Delfino, R. J. P., Lasco, R. D., Hilario, F. D., and Ares, E. D.: Observed
675   trends and impacts of tropical cyclones in the Philippines. International Journal of Climatology, 36(14). doi:10.1002/joc.4659,
2016.

Comiso, J. C., Perez, G. P. , and Stock, L. V. : Enhanced Pacific Ocean Sea Surface Temperature and Its Relation to Typhoon
Haiyan. Journal of Environmental Science and Management 18 (1): 1-10 https://ovcre.uplb.edu.ph/journals-
680   uplb/index.php/JESAM/article/view/175, 2015.

Copernicus Climate Change Service (CS3): ERA5. https://confluence.ecmwf.int/pages/viewpage.action?pageId=74764925,
2017.

685   Corporal-Lodangco, I.L. and Leslie, L.M.: Climatology of Philippine tropical cyclone activity: 1945–2011. Int. J. Climatol.,
37: 3525-3539. doi:10.1002/joc.4931, 2017.

Cruz, F. and Narisma, G.: WRF simulation of the heavy rainfall over Metropolitan Manila, Philippines during tropical cyclone Ketsana: a sensitivity study. Meteorology and Atmospheric Physics, 128(4), 415–428. doi:10.1007/s00703-015-0425-x, 2016.

690

Cruz, F. T, Sasaki, H., and Narisma, G.: Assessing the Sensitivity of the Non-Hydrostatic Regional Climate Model to Boundary Conditions and Convective Schemes over the Philippines, Journal of the Meteorological Society of Japan. 94A, 165-179 doi:10.2151/jmsj.2015-059, 2016.

695   Daron, J., Macadam, I, Kanamaru, H., Cinco, T., Katzfey, J., Scannell, C., … Tangang, F.: Providing future climate projections using multiple models and methods: insights from the Philippines. Climatic Change, 148(1–2). doi:10.1007/s10584-018-2183-5, 2018.

Di, Z., Gong, W., Gan, Y., She, C., and Duan, Q.: Combinatorial Optimization for WRF Physical Parameterization Schemes :
700   A Case Study of Three-Day Typhoon Simulations over the Northwest Pacific Ocean. doi:10.3390/atmos10050233%U, 2019.

Donelan, M. A., Haus, B. K., Reul, N., Plant, W. J., Sti- assnie, M., Graber, H. C., Brown, O. B., and Saltzman, E. S.: On the limiting aerodynamic roughness of the ocean in very strong winds, Geophys. Res. Lett., 31, L18306, doi:10.1029/2004GL019460, 2004.

705

Duc, T. Du, Duc, C. H., Hole, L. R., Hoang, L., Luong, H., Thanh, T., and Khanh, H. M.: Impacts of Different Physical Parameterization Configurations on Widespread Heavy Rain Forecast over the Northern Area of Vietnam in WRF-ARW Model, Adv. In Met. doi:10.1155/2019/1010858, 2019.

710   Dudhia, J.: Numerical study of convection observed during the Winter Monsoon Experiment using a mesoscale two–dimensional model. J. Atmos. Sci., 46, 3077–3107. doi:10.1175/1520-0469(1989)046<3077:NSOCOD>2.0.CO;2, 1989.

Eckstein, D., Künzel, V., Schäfer, L., and Winges, M. Global Climate Risk Index 2020 Who Suffers Most from Extreme Weather Events? Weather-Related Loss Events in 2018 and 1999 to 2018. https://www.germanwatch.org/en/17307, 2020.

715   Emanuel, K: Increasing destructiveness of tropical cyclones over the past 30 years. Nature 436, 686–688. doi:10.1038/nature03906, 2005.

EM-DAT: The Emergency Events Database - Université Catholique de Louvain (UCL) - CRED, D. Guha-Sapir, Brussels, Belgium. [Last database update: 30 June 2020.] http://www.emdat.be, 2020.

720

Flores, R. A.: Geovisual Analytics on the verification of the PAGASA Numerical Weather Prediction Model Rainfall Forecast, Int. Arch. Photogramm. Remote Sens. Spatial Inf. Sci., XLII-4/W19, 215–222, doi:10.5194/isprs-archives-XLII-4-W19-215-2019, 2019.

725   Gallo, F., Daron, J., Macadam, I., Cinco, T., Villafuerte, M., Jones, R. G., … Tucker, S.: High-resolution regional climate model projections of future tropical cyclone activity in the Philippines, 1181–1194. doi:10.1002/joc.5870, 2019.

Garratt, J.R.: Review: the atmospheric boundary layer, Earth-Science Reviews,37:1–2, 89-134, doi:10.1016/0012-8252(94)90026-4, 1994.

730

Glisan, J. M., W. J. Gutowski, J. J. Cassano, and Higgins, M. E.: Effects of Spectral Nudging in WRF on Arctic Temperature and Precipitation Simulations. J. Climate, 26, 3985–3999, doi:10.1175/JCLI-D-12-00318.1, 2013.

Green, B. W., and Zhang F.: Impacts of Air–Sea Flux Parameterizations on the Intensity and Structure of Tropical Cyclones.
735   Mon. Wea. Rev., 141, 2308–2324, doi:10.1175/MWR-D-12-00274, 2013.

Guo, X. : The Use of a Spectral Nudging Technique to Determine the Impact of Environmental Factors on the Track of Typhoon Megi (2010) *Atmosphere*, *8*(12), 257; doi:10.3390/atmos8120257, 2017.

740   Hashimoto, A., Done, J.M., Fowler, L.D. and Bruyère, C.L.: Tropical cyclone activity in nested regional and global grid-refined simulations. Climate Dynamics., 47, 497–508. doi:10.1007/s00382-015-2852-2, 2015.

Heming, J.T.: Tropical cyclone tracking and verification techniques for Met Office numerical weather prediction models. Meteorological Applications. doi:10.1002/met.1599, 2017.
745

Hennermann,   K.:   ERA5:   uncertainty   estimation
https://confluence.ecmwf.int/display/CKB/ERA5%3A+uncertainty+estimation, 2018.

Hersbach, H., Bell, B., Berrisford, P., Hirahara, S., Horányi, A., Nicolas, J., … Thépaut, J.: The ERA5 global reanalysis, Q J
750   R Meteorol Soc. 2020; 146: 1999– 2049. doi:10.1002/qj.3803, 2020.

Hill, K. A., and Lackmann, G. M.: Influence of Environmental Humidity on Tropical Cyclone Size, Mon Weather Rev 137(10), 3294-331 doi:10.1175/2009MWR2679.1, 2009.

755   Hodges, K.I.: Feature tracking on the unit sphere. Mon Weather Rev 123:3458–3465. doi:10.1175/1520-0493(1995)123%3c345 8:FTOTU S%3e2.0.CO;2, 1995.

Hodges, K.I.: Spherical nonparametric estimators applied to the UGAMP model integration for AMIP. Mon Weather Rev 124:2914–2932. doi:10.1175/1520- 0493(1996)124%3c291 4:SNEAT T%3e2.0.CO;2, 1996.
760

Hodges, K.I.: Adaptive constraints for feature tracking. Mon Weather Rev 127:1362–1373. doi:10.1175/1520-0493(1999)127%3c136 2:ACFFT %3e2.0.CO;2, 1999.

Hodges, K. I. and Klingaman, N. P. : Prediction errors of tropical cyclones in the western north Pacific in the Met Office global
765   forecast model. Weather and Forecasting, 34 (5). pp. 1189-1209. ISSN 0882-8156, doi:10.1175/WAF-D-19-0005.1, 2019.

Holden, W. N. : Typhoons, Climate Change, and Climate Injustice in the Philippines, 11(November 2015), 117–139.

Holland, G.J., J.M. Done, M. Ge, and R. Douglas, 2016: An Index for Cyclone Damage Potential.
770   https://ams.confex.com/ams/32Hurr/webprogram/Paper293660.html, 2018.

Hong, S-Y., Lim, J-OJ.: The WRF single-moment 6-class microphysics scheme (WSM6). J Korean Meteor Soc 42:129–151, 2006.

775   Hong, S-Y., Lim, K-SS., Kim, J-H., Lim, J-OJ., and Dudhia, J.: Sensitivity study of cloud-resolving convective simulations with WRF Using two bulk microphysical parameterizations: icephase microphysics versus sedimentation effects. J Appl Meteorol Clim 48:61–76, 2009.

Hong, S-Y., Noh, Y., and Dudhia J: A new vertical diffusion package with an explicit treatment of entrainment processes.
780   Mon Weather Rev 134:2318–2341, 2006.

Huffman, G.J., Stocker, E.F. , Bolvin, D.T. , Nelkin, E.J., and Tan, J.: GPM IMERG Final Precipitation L3 Half Hourly 0.1 degree x 0.1 degree V06, Greenbelt, MD, Goddard Earth Sciences Data and Information Services Center (GES DISC), doi:10.5067/GPM/IMERG/3B-HH/06, 2019.

785

IPCC: Summary for Policymakers. In: Climate Change 2013: The Physical Science Basis. Contribution of Working Group I to the Fifth Assessment Report of the Intergovernmental Panel on Climate Change [Stocker, T.F., D. Qin, G.-K. Plattner, M. Tignor, S.K. Allen, J. Boschung, A. Nauels, Y. Xia, V. Bex and P.M. Midgley (eds.)]. Cambridge University Press, Cambridge, United Kingdom and New York, NY, USA, 2013.

790

Isaksen, L., Bonavita, M., Buizza, R., Fisher, M., Haseler, J., Leutbecher, M. and Raynaud, L.: Ensemble of Data Assimilations at ECMWF. Technical Memorandum 636, ECMWF, Reading, UK. https://www.ecmwf.int/en/elibrary/10125-ensemble-data-assimilations-ecmwf, 2010.

795   Islam, T., Srivastava, P.K., Rico-Ramirez, M.A. et al.: Tracking a tropical cyclone through WRF–ARW simulation and sensitivity of model physics. Nat Hazards 76, 1473–1495, doi:10.1007/s11069-014-1494-8, 2015.

Japan Meteorological Agency (JMA): Annual Report 2013. https://www.jma.go.jp/jma/jma-eng/jma-center/rsmc-hp-pub-g/AnnualReport/2013/Text/Text2013.pdf, 2013.

800

Jin C.S., Cha D.H., Lee D.K., Suh M-S,. Hong S.Y., Kang H.S., Ho C.H: Evaluation of climatological tropical cyclone activity over the western North Pacific in the CORDEX-East Asia multi-RCM simulations. Clim Dyn, https: doi:10.1007/s00382-015-2869-6, 2015.

805   Judt, F., Klocke, D., Rios-Berrios, R., et al.,: Tropical Cyclones in Global Storm-Resolving Models, Journal of the Meteorological Society of Japan. 2021-029, , doi:10.2151/jmsj.2021-029, 2021.

Kain, J.S.: Convective parameterization for mesoscale models: the Kain Fritsch scheme. The representation of cumulus convection in numerical models. Meteorol. Monogr. 46, 165–170. doi:10.1007/978-1-935704-13-3_16, 1993.

810

Kain, J.S.: The Kain–Fritsch convective parameterization: an update. J. Appl. Meteorol. Climatol. 43, 170–181. Doi:10.1175/1520-0450(2004)043<0170:TKCPAU>2.0.CO;2, 2004.

Natural Hazards
and Earth System
Sciences
Discussions

Kimura, F. and Kitoh, A.: Downscaling by Pseudo Global Warning Method. https://www.chikyu.ac.jp/P-
815   C09/ICCAP/ICCAP_Final_Report/2/4-climate_kimura.pdf, 2007.

Knapp, K. R., Knaff, J. A., Sampson, C. R., Riggio, G. M., and Schnapp, A. D.: A pressure-based analysis of the historical
western North Pacific tropical cyclone intensity record, Mon. Weather Rev., 141, 2611—2631, doi:10.1175/MWR- D-12-
00323.1, 2013.

820

Knapp, K.R., Applequist, S., Diamond, H.J., Kossin, J.P., Kruk, M., and Schreck, C.: NCDC International Best Track Archive
for Climate Stewardship (IBTrACS) Project, Version 3. NOAA National Centers for Environmental Information.
doi:10.7289/V5NK3BZP, 2019.

825   Knutson, T., and Coauthors: Tropical Cyclones and Climate Change Assessment: Part II: Projected Response to Anthropogenic
Warming. Bull. Amer. Meteor. Soc., 101, E303–E322, doi:10.1175/BAMS-D-18-0194.1, 2020.
Knutson, T., Camargo, S. J., Chan, J. C. L., Emanuel, K., and Ho, C.: Tropical Cyclones and Climate Change Assessment:
Part I . Detection and Attribution, 1–61. doi:10.1175/BAMS-D-18-0189.1, 2020.

830   Kubota, H., and Chan, J.C.L.: Interdecadal variability of tropical cyclone landfall in the Philippines from 1902 to 2005.
Geophys. Res. Lett. 36: L12802, doi:10.1029/2009GL038108, 2009.

Kueh, M.-T., Chen, W.-M., Sheng, Y.-F., Lin, S. C., Wu, T.-R., Yen, E., Tsai, Y.-L., and Lin, C.-Y.: Effects of horizontal
resolution and air–sea flux parameterization on the intensity and structure of simulated Typhoon Haiyan (2013), Nat. Hazards
835   Earth Syst. Sci., 19, 1509–1539, doi:10.5194/nhess-19-1509-2019, 2019.

Kueh, M.-T.: Multiformity of the tropical cyclone wind–pressure relationship in the western North Pacific: Discrepancies
among four best-track archives, Environ. Res. Lett., 7, 024015, doi:10.1088/1748-9326/7/2/024015, 2012.

840   Lagmay, A.M.F., Agaton, R.P., Bahala, M.A.C., Briones, J.B.L.T., Cabacaba, K.M.C., Caro, C.V.C., Dasallas, L.L., Gonzalo,
L.A.L., Ladiero, C.N., Lapidez, J.P., Mungcal, M.T.F., Puno, J.V.R., Ramos, M.M.A.C., Santiago, J., Suarez, J.K., Tablazon,
J.P..: Devastating storm surges of Typhoon Haiyan. Int. J. Disaster Risk Red. 11:1–12, doi:10.1016/j.ijdrr.2014. 10.006,2015.

Lander, M., Guard, C., and Camargo, S.: Super Typhoon Haiyan, in: State of the Climate in 2013, B. Am. Meteorol. Soc., 95,
845   S112– S114, 2014.

Lee TC, Knutson TR, Kamahori H, Ying M.: Impacts of Climate Change on Tropical Cyclones in the Western North Pacific
Basin. Part I: Past Observations. Tropical Cyclone Res. Rev. 1:213–230. doi:10.6057/2012TCRR02.08, 2012.

850   Lee, JD., and Wu, CC.:The Role of Polygonal Eyewalls in Rapid Intensification of Typhoon Megi (2010), 4175–4199.
doi:10.1175/JAS-D-18-0100.1, 2018.

Li, F., Song, J. & Li, X.: A preliminary evaluation of the necessity of using a cumulus parameterization scheme in high-
resolution simulations of Typhoon Haiyan (2013). Nat Hazards 92, 647–67. doi:10.1007/s11069-018-3218-y, 2018.

855

Lyon, B and Camargo S.J.: The seasonally-varying influence of ENSO on rainfall and tropical cyclone activity in the Philippines. Clim. Dyn. 32:125–141, doi:10.1007/s00382-008-0380-z, 2009.

McSweeney, C,. Jones, R., Booth, B.: Selecting ensemble members to provide regional climate change information. J Clim 860   25:7100–21. doi:10.1175/JCLI-D-11-00526.1, 2012.

McSweeney, C., Jones, R., Lee, R., Rowell, D.: Selecting CMIP5 GCMs for downscaling over multiple regions. Clim Dyn 44(11-12):3237-3260. doi:10.1007/s00382-014-2418-8, 2015.

865   Mesoscale and Microscale Meteorology Laboratory – National Center for Atmospheric Research (MMML-NCAR): Weather Research and Forecasting Model, ARW Version 4 Modeling System User's Guide. https://www.mmm.ucar.edu/weather-research-and-forecasting-model, 2019.

Mittal, R., Tewari, M., Radhakrishnan, C., Ray, P., and Singh, T.: Response of tropical cyclone Phailin (2013) in the Bay of 870   Bengal to climate perturbations. Climate Dynamics, (2013). doi:10.1007/s00382-019-04761,2019.

Mlawer, Eli. J., Steven. J. Taubman, Patrick. D. Brown, M. J. Iacono, and S. A. Clough: Radiative transfer for inhomogeneous atmospheres: RRTM, a validated correlated–k model for the longwave. J. Geophys. Res., 102, 16663–16682. doi:10.1029/97JD00237, 1997.

875

Mohandas, S. and Ashrit, R.: Sensitivity of different convective parameterization schemes on tropical cyclone prediction using a mesoscale model. Nat Hazards 73, 213–235 (2014). doi:10.1007/s11069-013-0824-6, 2014.

Mohanty, U. C., Osuri, K. K., Routray, A., Mohapatra, M., and Pattanayak, S.: Simulation of bay of bengal tropical cyclones 880   with wrf model: Impact of initial and boundary conditions. Marine Geodesy, 33(4), 294–314. doi:10.1080/01490419.2010.518061, 2010.

Monin A. S., and A. M. Obukhov: Basic laws of turbulent mixing in the surface layer of the atmosphere. Contrib Geophys Inst Acad Sci USSR 151:163–187, https://gibbs.science/efd/handouts/monin_obukhov_1954.pdf, 1954.

885

Moon, J., Cha, D.-H., Lee, M., & Kim, J. : Impact of spectral nudging on real-time tropical cyclone forecast. Journal of Geophysical Research: Atmospheres, 123, 12,647– 12,660. doi:10.1029/2018JD028550, 2018.

Mori, N., Kato, M., Kim, S., Mase, H., Shibutani, Y., Takemi, T., Tsuboki, K., and Yasuda, T.: Local amplification of storm 890   surge by Super Typhoon Haiyan in Leyte Gulf. Geophysical Research Letters, Volume 41, Issue 14, Pages 5106-5113. doi:10.1002/2014GL060689, 2014.

Nakamura, R., Shibayama, T., Esteban, M. and Iwamoto, T.: Future typhoon and storm surges under different global warming scenarios: case study of typhoon Haiyan (2013). Nat. Hazards, 82, 1645-1681. doi:10.1007/s11069-016-2259-3, 2016.

895

National Disaster Risk Reduction and Management Council (NDRRMC): NDRRMC situational reports. http://www.ndrrmc.gov.ph/ (accessed 2 February 2020), 2020.

PAGASA: Observed and projected climate change in the Philippines. PAGASA, Quezon City, Philippines, 36pp, Available
900   from
https://pubfiles.pagasa.dost.gov.ph/iaas/FINAL_observed_climate_trends_and_projected_climate_change_in_the_Phils_2018.
pdf , 2018.

Parker, C.L., Bruyère, C.L., Mooney, P.A. et al.: The response of land-falling tropical cyclone characteristics to projected
905   climate change in northeast Australia. Clim Dyn 51, 3467–3485, doi:10.1007/s00382-018-4091-9, 2018.

Parker, C. L., Lynch, A. H., and Mooney, P. A.: Factors affecting the simulated track and intensification of Tropical Cyclone
Yasi (2011), 194(November 2016), 27–42. doi:10.1016/j.atmosres.2017.04.002, 2017.

910   Patricola, C. M., and Wehner, M. F: Article Anthropogenic influences on major tropical cyclone events. Nature.
doi:10.1038/s41586-018-0673-2, 2018.

Peng, X., Fei, J., Huang, X., and Cheng, X. : Evaluation and Error Analysis of Official Forecasts of Tropical Cyclones during
2005–14 over the Western North Pacific. Part I: Storm Tracks, Weather and Forecasting, 32(2), 689-712. Retrieved Apr 28,
915   2021, from https://journals.ametsoc.org/view/journals/wefo/32/2/waf-d-16-0043_1.xml, 2017.

Potty, J., Oo, S. M., Raju, P. V. S., and Mohanty, U. C.: Performance of nested WRF model in typhoon simulations over West
Pacific and South China Sea. Natural Hazards, 63(3), 1451–1470. doi:10.1007/s11069-011-0074-4,2012.

920   Powell, M. D., Vickery, P. J., and Reinhold, T. A.: Reduced drag coefficient for high wind speeds in tropical cyclones, Nature,
24, 395–419, doi:10.1038/nature01481, 2003.

Powers, J.G., C.L. Bruyère, J.M. Done, J. Dudhia, T.J. Galarneau, Jr., M.J. Kavulich, Jr., S.E. Peckham, and W. Wang.: The
Weather Research and Forecasting Model and Its Applications. Meteor. Technology Int'l., April 2014, 30-33.
925   Doi:10.1175/BAMS-D-15-00308.1, 2014.

Powers, J.G., J.B. Klemp, W.C. Skamarock, C.A. Davis, J. Dudhia, D.O. Gill, J.L. Coen, D.J. Gochis, R. Ahmadov, S.E.
Peckham, G.A. Grell, J. Michalakes, S. Trahan, S.G. Benjamin, C.R. Alexander, G.J. Dimego, W. Wang, C.S. Schwartz, G.S.
Romine, Z. Liu, C. Snyder, F. Chen, M.J. Barlage, W. Yu, and M.G. Duda: The Weather Research and Forecasting Model:
930   Overview, System Efforts, and Future Directions. Bull. Amer. Meteor. Soc., 98, 1717–1737,
doi:10.1175/BAMS-D-15-00308.1, 2017.

Prater, B., Evans, J.: Sensitivity of modeled tropical cyclone track and structure of hurricane Irene (1999) to the convective
parameterization scheme. Meteorol Atmos Phys 80, 103–115. doi:10.1007/s007030200018, 2002.
935

Sato, T., Kimura, F., Kitoh, A.: Projection of Global Warming onto Regional Precipitation over Mongolia Using a Regional
Climate Model. Journal of Hydrology 333(1):144-154. doi:10.1016/j.jhydrol.2006.07.023, 2007.

Satya, O. C., Mandailing, P. M., and Kaban, H.: Application of advanced research WRF model using tropical (New TK)
940   scheme and KF scheme in predicting short-term weather in Palembang and its surrounding areas Application of advanced

Natural Hazards
and Earth System
Sciences
Discussions

research WRF model using tropical (New TK) scheme and KF scheme in predicting short-term weather in Palembang and its surrounding areas. doi:10.1088/1742-6596/1282/1/012025, 2019.

Scoccimarro, E.: Modeling Tropical Cyclones in a Changing Climate. Oxford Research Encyclopedias: Natural Hazard
945   Science, DOI:10.1093/acrefore/9780199389407.013.2, 2016.

Shen, W., Song, J., Liu, G., Zhuang, Y., Wang, Y., Tang, J.: The effect of convection scheme on tropical cyclones simulations over the CORDEX East Asia domain. Clim Dyn 52:4695–4713. doi:/10.1007/s0038 2-018-4405-y, 2019.

950   Shen, W., Tang, J., Wang, Y., Wang, S., and Niu, X.: Evaluation of WRF model simulations of tropical cyclones in the western North Pacific over the CORDEX East Asia domain. Climate Dynamics, 48(7), 2419–2435. doi:10.1007/s00382-016-3213-5, 2017.

Shepherd, T. J., and Walsh, K. J.: Sensitivity of hurricane track to cumulus parameterization schemes in the WRF model for
955   three intense tropical cyclones: impact of convective asymmetry. Meteorog. Atmos. Phys., 129(4), 345–374. doi:10.1007/s00703-016-0472-y, 2017.

Shimada, U., Kubota, H., Yamada, H., Cayanan, E. O., and Hilario, F. D.: Intensity and Inner-Core Structure of Typhoon Haiyan (2013) near Landfall: Doppler Radar Analysis, Mon. Weather Rev. 146(2), 583-597.doi:10.1175/MWR-D-17-0120.1,
960   2018.

Skamarock, W.C., Klemp, J.B., Dudhia, J., Gill, D.O., Barker, D.M., Duda, M., Huang, X-Y., Wang, W., Powers, J.G.: A description of the advanced research WRF version 3. NCAR Technical Note, NCAR/TN-475?STR, National Center for Atmospheric Research, Boulder, Colorado, 2008.

965

Soria, J. L. A., Switzer, A. D., Villanoy, C. L., Fritz, H. M., Bilgera, P. H. T., Cabrera, O. C., Siringan, F. P., Maria, Y. Y., Ramos, R. D., and Fernandez, I. Q.: Repeat Storm Surge Disasters of Typhoon Haiyan and Its 1897 Predecessor in the Philippines, Bulletin of the American Meteorological Society, 97(1), 31-48. Doi:/10.1175/BAMS-D-14-00245.1, 2016.

970   Spencer P, Shaw B, Pajuelas B. 2012. Sensitivity of typhoon Parma to various WRF model configurations. In Technical Report on 92nd American Meteorological Society Annual Meeting, 26 January 2012, New Orleans, LA; 608–619. American Meteorological Society: Boston, MA. 2012.

Takayabu, I., Hibino, K., Sasaki, H., Shiogama, H., Mori, N., Shibutani, Y. and Takemi, T.: Climate change effects on the
975   worst-case storm surge: a case study of Typhoon Haiyan, Environ. Res. Lett. 10 089502. doi:10.1088/1748-9326/10/6/064011, 2015.

Tang, J., Wang, S., Niu, X., Hui, P., and Zong, P.: Impact of spectral nudging on regional climate simulation over CORDEX East Asia using WRF. Climate Dynamics, 48(7), 2339–2357. doi:10.1007/s00382-016-3208-2, 2017.

980

Tewari, M., F. Chen, W. Wang, J. Dudhia, M. A. LeMone, K. Mitchell, M. Ek, G. Gayno, J. Wegiel, and R. H. Cuenca: Implementation and verification of the unified NOAH land surface model in the WRF model. 20th conference on weather

analysis and forecasting/16th conference on numerical weather prediction, pp. 11–15, https://ams.confex.com/ams/84Annual/techprogram/paper_69061.htm 2004.

985

Tiedtke, M.: A Comprehensive Mass Flux Scheme for Cumulus Parameterization in Large-Scale Models, Mon. Weather Rev. 117(8), 1779-1800. doi:10.1175/1520-0493(1989)117<1779:ACMFSF>2.0.CO;2,1989,

Torn, R.D., and Davis, D.A.: The influence of shallow convection on tropical cyclone track forecasts. Mon. Weather Rev. 140,
990 2188–2197, doi:10.1175/MWR-D-11-00246., 2012.

Tolentino, J.T. and Bagtasa, G.:Calibration of Kain–Fritsch cumulus scheme in Weather Research and Forecasting (WRF) model over Western Luzon, Philippines. Meteorol Atmos Phys, doi:10.1007/s00703-021-00779-0, 2021.

995 Villafuerte, M. Q., John, I. I., Lambrento, C. R., Hodges, K. I., Cruz, F. T., Cinco, T. A., and Narisma, G. T.: Sensitivity of tropical cyclones to convective parameterization schemes in RegCM4. Climate Dynamics, (0123456789). doi:10.1007/s00382-020-05553-3, 2021.

Wada, A.: Effect of Air-Sea Environmental Conditions and Interfacial Processes on Extremely Intense Typhoon Haiyan
1000 (2013), 379–405. doi:10.1029/2017JD028139, 2018.

Walsh, K.J.E., McBride, J.L., Klotzbach, P.J., Balachandran, S., Camargo, S.J., Holland, G., Knutson, T.R., Kossin, J.P., Lee, T., Sobel, A. and Sugi, M.: Tropical Cyclones and Climate Change. WIREs Clim Change 2015. doi:10.1002/wcc.371, 2015.

1005 Walsh K.J.E., S.J. Camargo, T.R. Knutson, J. Kossin, T.-C. Lee, H. Murakami, C. Patricola, Tropical cyclones and climate change, Tropical Cyclone Research and Review, Volume 8, Issue 4, 2019, Pages 240-250, ISSN 2225-6032, doi:10.1016/j.tcrr.2020.01.004, 2019.

Wang, H., Wang, Y. and Xu, H.: Improving simulation of a tropical cyclone using dynamical initialization and large-scale
1010 spectral nudging: A case study of Typhoon Megi (2010). Acta Meteorol Sin 27, 455–475, doi:10.1007/s13351-013-0418-y, 2013.

Xue, F., and F. X. Fan.: Anomalous western Pacific subtropical high during late summer in weak La Niñayears: Contrast between 1981 and 2013. Adv. Atmos. Sci., 33(12), 1351–1360, doi:10.1007/s00376-016-5281-1, 2016.

1015 Yavinchan, S., Exell, R. H. B., and Sukawat, D.: Precipitation Forecasts by the New KF Convective Parameterization Scheme during the Extreme Precipitation Event in Southern Thailand 2. 21–24., https://www.thaiscience.info/Article%20for%20ThaiScience/Article/61/10011022.pdf, 2006.

Yesubabu, V., Srinivas, C. V, Ramakrishna, S. S. V. S., and Prasad, K. B. R. R. H.: Impact of period and timescale of FDDA
1020 analysis nudging on the numerical simulation of tropical cyclones in the Bay of Bengal, 2109–2128. doi:10.1007/s11069-014-1293-2, 2014.

Yonson, R., Gaillard, J. C., and Noy, I.: The measurement of disaster risk : An example from tropical cyclones in the Philippines Rio Yonson , J C Gaillard and Ilan Noy. Review of Development Economics, 2(22), 736–765., 2016.

1025

Zhang, C., Wang, Y., Hamilton, K.: Improved representation of boundary layer clouds over the Southeast Pacific in ARW-WRF using a modified TK cumulus parameterization scheme. Mon. Weather Rev. 139 (11), 3489–3513. Doi:10.1175/MWR-D-10-05091.1 .2011.

1030   Zhang, D.-L. and Chen, H.: Importance of the upper-level warm core in the rapid intensification of a tropical cyclone, Geophys. Res. Lett., 39, L02806, doi:10.1029/2011GL050578, 2012.

Zhang, J. A., Black, P. G., French, J. R., and Drennan, W. M.: First direct measurements of enthalpy flux in the hurricane boundary layer: The CBLAST results, Geophys. Res. Lett., 35, L14813, doi:10.1029/2008GL034374, 2008.